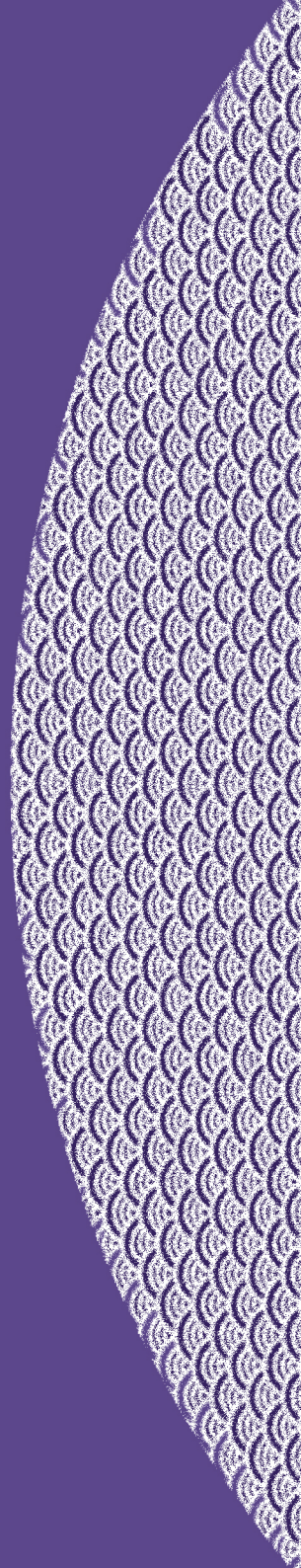


Pure and
Applied
Algebraic
Topology

My Ismail Mamouni



Pure and Applied Algebraic Topology

Pure and Applied Algebraic Topology

By

My Ismail Mamouni

**Cambridge
Scholars
Publishing**



Pure and Applied Algebraic Topology

By My Ismail Mamouni

This book first published 2022

Cambridge Scholars Publishing

Lady Stephenson Library, Newcastle upon Tyne, NE6 2PA, UK

British Library Cataloguing in Publication Data

A catalogue record for this book is available from the British Library

Copyright © 2022 by My Ismail Mamouni

All rights for this book reserved. No part of this book may be reproduced, stored in a retrieval system, or transmitted, in any form or by any means, electronic, mechanical, photocopying, recording or otherwise, without the prior permission of the copyright owner.

ISBN (10): 1-5275-7972-7

ISBN (13): 978-1-5275-7972-9

ALGEBRAIC TOPOLOGY PAGE 1

1	History	1
2	Functors and categories	2
3	Homology	3
4	Cohomology	10
5	Homotopy	12

RATIONAL HOMOTOPY THEORY PAGE 17

1	Introduction	17
2	Hilali Conjecture	19
3	Halperin Conjecture	24
4	Theriault Conjecture	26
5	Rational homotopy type classification	30

TOPOLOGICAL ROBOTICS PAGE 33

1	Introduction	33
2	Topology of motion planning algorithms	34
3	Loop topological complexity	35
4	String Topological Robotics	38

TOPOLOGICAL DATA ANALYSIS _____ **PAGE 49** _____

1	Introduction	49
2	Persistent homology	50
3	Images Recognition	54
4	Neuronal sciences	62
5	Machine learning	72
6	Linguistics	83

APPLIED CATEGORY THEORY _____ **PAGE 91** _____

1	Glossary	91
2	Dynamical systems (Ongoing Works)	92

BIBLIOGRAPHY _____ **PAGE 93** _____

Chapter 1

Algebraic Topology

1

History

For many people, Poincaré's works [59] are the real foundation of the algebraic topology, when he defined for the first time in 1905 what is meant by homologous chains in a manifold. His definition was rather imprecise, but the notion he used covered exactly the current acceptance: two closed chains are homologous if they differ by an edge.

By 1940, the homological algebra theory was well defined and contributed greatly to the emergence of many other concepts like categories and functors. Various generalisations have been imagined later, like cohomology of groups with many surprising geometrical connections, bounded cohomology and equivariant cohomology. This shows, how homological notions have become largely widespread in almost all mathematics areas, and sometimes even in theoretical physics. The main principle of algebraic topology is to associate, in a functorial way, to any topological object an algebraic object which is invariant under certain kinds of transformations like homeomorphisms, homotopisms, holomorphisms and isomorphisms.

A constructive example is how to apply to a torus, two scissors to make it homeomorphic to a paper sheet. Topologically speaking,

scissors here symbolise loops. Two cuts are said to be equivalent, when they have the same effect on the ambient space. In other words one can continuously switch from one to the other. The first cut goes around the central hole; and we get a crown. The second one is a radial cut on this crown and gives us a rectangle.

2

Functors and categories



Definition 1.1

A *category* is a collection of objects connected by a kind of arrows, called *morphisms* such that

1. $(f \circ g) \circ h = f \circ (g \circ h)$, for any morphisms f, g, h , whenever the composition is possible;
2. For any object X , there exists an unique morphism, denoted $id_X \in \text{hom}(X, X)$ such that $id_X \circ f = f \circ id_X = f$, for any other morphism f , whenever the composition is possible.

As example of categories, one may consider sets connected by maps, topological spaces connected by continuous maps, groups connected by morphisms of groups, or finally vector spaces connected by linear maps.



Definition 1.2

A *functor* T between two given categories \mathcal{C} and \mathcal{C}' is any correspondence

$$T: \mathcal{C} \longrightarrow \mathcal{C}'$$

that associates to any object X in \mathcal{C} , an object $T(X)$ in \mathcal{C}' , and associates to any morphism $f: X \longrightarrow Y$ in \mathcal{C} , a morphism $T(f): T(X) \longrightarrow T(Y)$ in \mathcal{C}' , such that

$$T(id_X) = id_{T(X)},$$

• for any X in \mathcal{C} .

Vocabulary. Let $T: \mathcal{C} \rightarrow \mathcal{C}'$ be a functor.

- T is said to be covariant when $T(f \circ g) = T(f) \circ T(g)$, for any f, g ;
- T is said to be contravariant when $T(f \circ g) = T(g) \circ T(f)$, for any f, g ;

Examples.

1. Let $\mathcal{C} = Gpe$, be the category of groups endowed with morphisms of groups, then $T(g) = g^{-1}$ is a contravariant functor.
2. Let $\mathcal{C} = Gpe$, be the category of groups endowed with morphisms of groups, then $T(g) = h^{-1}.g.h$ is a covariant functor, where h is a fixed morphism.

3

Homology



Definition 1.3

A *chain complex* is any \mathbb{N} -indexed family $(C_n)_{n \in \mathbb{N}}$ of modules endowed with a family of morphisms of modules

$$d_n: C_n \longrightarrow C_{n-1},$$

such that

$$d_n \circ d_{n+1} = 0,$$

with the convention that $C_{-1} = 0$.

Following the notation here above, $Z_n := \text{Im}d_{n+1} \subset B_n := \ker d_n$. Elements of Z_n are called *n-cycles*, while those of B_n are called *n-bords*. From $Z_{n+1} := \text{Im}d_{n+1} \subset B_n := \ker d_n$, we deduce that any cycle is a bord. The inverse is naturally not always true.

By setting $C := \bigoplus_{n \in \mathbb{N}} C_n$, we get a graduation: any element $c \in C_n$ is called of degree n and we write $|c| = n$. This yields to the map

$d: C \rightarrow C$ where $d|_{C_n} = d_n$. In particular $d^2 = 0$, which means that d is a derivation, called a *differential*.

Definition 1.4

Let $(C, d) = \bigoplus_{n \in \mathbb{N}} C_n$ a chain complex.

- $H_n(C, d) = \ker d_n / \text{Im } d_{n+1}$ is called the n -th group of homology of (C, d) ;
- $\beta_n(C) = \text{rank } H_n(C, d)$ is called the Betti number of (C, d) ;
- $H_*(C, d) = \bigoplus_{n \in \mathbb{N}} H_n(C, d)$ is the homology group of (C, d) ;
- $\dim H_*(C, d) = \sum_{n=0}^{+\infty} \beta_n(C)$ is the homological dimension of (C, d) ;
- $\chi_c(C) = \sum_n (-1)^n \beta_n(C)$ is the Euler-Poincaré homological invariant of (C, d) .

It is worth pointing out that the homology measures the obstruction of a bond to be a cycle. In fact, two bords x and y are homologous, i.e., $[x] = [y]$, means that $dx = dy = 0$ and that $x = y + dc$.

Definition 1.5

Let n be a fixed integer. A standard n -simplex (or standard simplex of dimension n) in \mathbb{R}^n , denoted generally Δ_n , is the hull convex in \mathbb{R}^n of the points e_0, e_1, \dots, e_n , where $e_0 = (0, \dots, 0)$, $e_1 = (1, 0, \dots, 0)$, \dots , and $e_n = (0, \dots, 0, 1)$.

- A 0-standard simplex is a point;
- A 1-standard simplex is a segment;
- A 2-standard simplex is a full triangle;



Figure 1.1: A tetrahedron is 3-simplex

- A 3-standard simplex is a full tetrahedron.

Definition 1.6

Let n be a fixed integer, and Δ a given n -standard simplex. Let $0 \leq k \leq n$. Any hull convex of a sub-family (e_i) of k elements among e_0, e_1, \dots, e_n is a k -standard simplex of Δ , called a k -face of Δ .

For example, the 0-faces of a tetrahedron are its vertices, its 1-faces are its edges, while its 2-faces are its full triangles. The table here above summarises the number of faces of some examples of n -simplices

simplex	0-faces	1-faces	2-faces	3-faces	4-faces	5-faces
Point	1	-	-	-	-	-
Segment	2	1	-	-	-	-
Triangle	3	3	1	-	-	-
Tetrahedron	4	6	4	1	-	-
Pentachord	5	10	10	5	1	-
5-simplex	6	15	20	15	6	1
6-simplex	7	21	35	35	21	7

We get this Euler-Poincaré formula:

$$\sum_{n \geq 0} (-1)^n r_n(C) = 1,$$

where r_n denotes the number of the n -faces in C .

§ Definition 1.7

We call a *simplicial complex* any set of simplices \mathcal{K} , that satisfies the following conditions:

1. Every face of a simplex from \mathcal{K} is also in \mathcal{K} ;
2. Any non empty intersection of two simplices $\sigma_1, \sigma_2 \in \mathcal{K}$ is a face of both σ_1 and σ_2 .

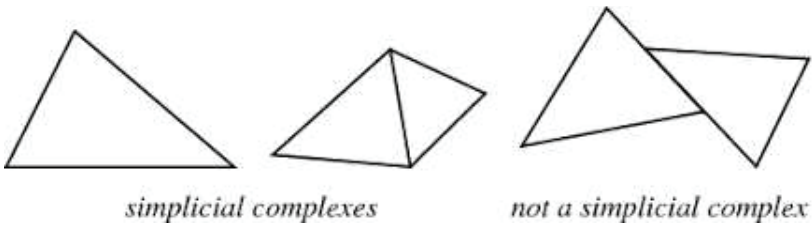


Figure 1.2: Simplicial complex or not?

§ Definition 1.8

Let \mathcal{K} be a simplicial complex, and n a fixed integer.

We call a *n-chain* in \mathcal{K} any formal sum $\sum n_i \sigma_i$, where σ_i are n -simplices in \mathcal{K} , with coefficients $n_i \in \mathbb{Z}$.

The subset of all this n -chains will be denoted $\mathcal{C}_n(\mathcal{K})$, with the convention that $\mathcal{C}_{-1}(\mathcal{K}) = \emptyset$.

§ Definition 1.9

Let \mathcal{K} be a simplicial complex.

The *boundary operator* on \mathcal{K} , is the \mathbb{Z} -linear map defined by:

$$\begin{aligned} \partial_n: \quad \mathcal{C}_n(\mathcal{K}) &\longrightarrow \mathcal{C}_{n-1}(\mathcal{K}) \\ \sigma := [e_0, \dots, e_n] &\longmapsto \partial_n \sigma \end{aligned}$$

where, $\partial_n \sigma = \sum_{i=0}^n (-1)^i [e_0, \dots, \hat{e}_i, \dots, e_n]$ and that \hat{e}_i means omitted.

One can check that



Theorem 1.1

$$\partial_{n-1} \circ \partial_n = 0.$$

In particular we have

$$\text{Im} \partial_n \subset \ker \partial_{n-1}.$$

This yields the chain complex

$$0 \xleftarrow{i} C_n(\mathcal{K}) \xrightarrow{\partial_n} C_{n-1}(\mathcal{K}) \xrightarrow{\partial_{n-1}} \dots \xrightarrow{\partial_1} C_0(\mathcal{K}) \xrightarrow{\partial_0} 0,$$

which is an algebraic structure that consists of a sequence of abelian groups (or modules) and a sequence of homomorphisms between consecutive groups such that the image of each homomorphism is included in the kernel of the next. Elements of $\text{Im} \partial_k$ are called *boundaries*, those of $\ker \partial_{k-1}$ are called *cycles*. Thus any boundary is a cycle, the inverse is not always true.



Definition 1.10

The k -th simplicial *homology group* of \mathcal{K} , is defined to be the quotient group

$$H_k(\mathcal{K}) = \ker \partial_{k-1} / \text{Im} \partial_k.$$

Its rank, denoted $\beta_p(\mathcal{K})$, is called the k -th *Betti number* of \mathcal{K} .

$H_k(\mathcal{K})$ represents the obstruction of a cycle to be a boundary, and $\beta_p(\mathcal{K})$ represents the number of the homologous k -dimensional holes in a shape. Since the interior of a circle is a disc, which is a variety of dimension 1, one may consider a circle to have a one-dimensional hole. In particular β_0 is the number of the path-connected components of a shape, since two points are homotopic if and only if they live in the same path-connected component.

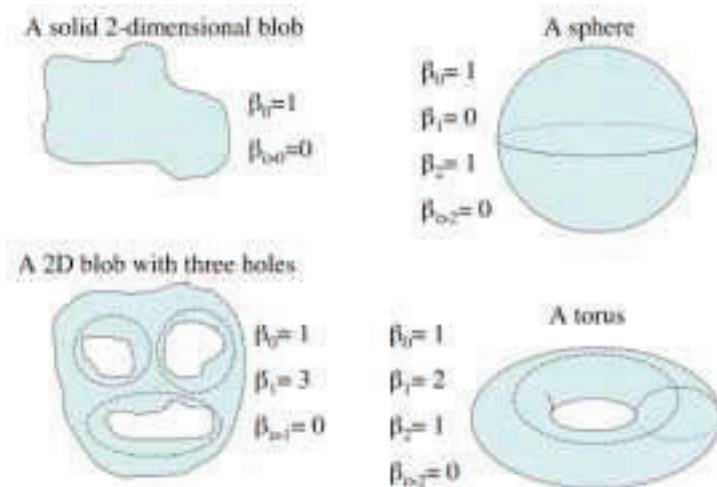


Figure 1.3: Betti numbers of some shapes.

Definition 1.11

Let X be a topological space, and n a fixed integer.

Any continuous map $\sigma: \Delta_n \rightarrow X$ is called a n -singular simplex of X .

While identifying σ to its geometrical image in X , it is clear that:

- 0-singular simplices are points of X ;
- 1-singular simplices are curves in X ;
- 2-singular simplices are 3D-surfaces in X ;
- 0-singular simplices are 3D-volumes in X .

Definition 1.12

Let X be a topological space, and n a fixed integer.

n -singular chains are all finite sums, $\sum n_i \sigma_i$, where n_i are integers, while σ_i are n -singular simplices.

- The \mathbb{Z} -module of such chains, will be denoted $C_n(X)$.



Definition 1.13

Let X be a topological space, and n a fixed integer. The bord operator $\partial: C_n(X) \rightarrow C_{n-1}(X)$ is defined by

$$\partial\sigma = \sum_{i=0}^n (-1)^i \sigma|_{\Delta_{n-1}^i},$$

where $\Delta_{n-1}^i = [e_0, \dots, \hat{e}_i, \dots, e_n]$ and that \hat{e}_i means omitted.



Theorem 1.2

Following the notations here above, we have

$$\partial^2 = 0$$

In particular we have

$$\text{Im } \partial_n \subset \ker \partial_{n-1}.$$

Hence, we obtain a chain complex

$$0 \xleftarrow{i} C_n(X) \xrightarrow{\partial_n} C_{n-1}(X) \xrightarrow{\partial_{n-1}} \dots \xrightarrow{\partial_1} C_0(X) \xrightarrow{\partial_0} 0,$$

whose homology is called the singular homology of X .



Definition 1.14

Let X be a topological space, and $C(X)$ its associated singular chain complex as described here above. Then, we put

$$H_*(X) := H_*(C(X), \partial), \text{ the singular homology of } X.$$



Remark 1.1

Let X and Y be two given topological spaces, and $f: X \rightarrow Y$ a continuous map. For any singular X -simplex $\sigma: \Delta_n \rightarrow X$, one can associate a singular Y -simplex: $f \circ \sigma: \Delta_n \rightarrow Y$. In particular, if σ_1 and σ_2 are two homologous cycles in X , then their images are still homologous in Y .

This enables us to define on the category **Top**, of topological spaces, endowed with continuous maps, the following invariant functor:

$$H_*: X \mapsto H_*(X), H_*: f \mapsto H_*(f)$$

where

$$\begin{aligned} H_*(f): H_*(X) &\longrightarrow H_*(Y) \\ [\sigma] &\longmapsto [f \circ \sigma] \end{aligned}$$

4

Cohomology



Definition 1.15

A cochain complex is any graded family $(C^n)_{n \in \mathbb{N}}$ of \mathbb{Z} -modules equipped with \mathbb{Z} -morphisms $d^n: C^n \rightarrow C^{n+1}$ such that $d^{n+1} \circ d^n = 0$.

By analogy to the above, we set $B^n := \text{Im} d^n \subset Z^{n+1} = \ker d^{n+1}$, and define the *cohomology* of (C, d) to be

$$H^n(C, d) := Z^{n+1} / B^n.$$

- Elements of Z^n are called *n-cocycles*;
- elements of B_n are called *n-cobords*.

For a given topological space, X , we dualize its singular homology as follows:

$$C^n(X) := C_n(X)^\#$$

and put

$$d := \partial^\#,$$

we get a cochain complex $C^*(X, d)$, whose cohomology is called the *singular cohomology* of X .

Definition 1.16

Let X be a fixed topological space. The *cap product* is the bilinear application defined as follows:

$$\begin{aligned} \frown : C_p(X; K) \times C^q(X; K) &\longrightarrow C_{p-q}(X; K) \\ (\sigma, \delta) &\longmapsto \sigma \frown \delta := \delta(\sigma|_{[e_0, \dots, e_q]})\sigma|_{[e_q, \dots, e_p]} \end{aligned} ,$$

that can be extended naturally to homology and cohomology as follows:

$$\frown : H_p(X; K) \times H^q(X; K) \longrightarrow H_{p-q}(X; K).$$

If X is a closed and orientable manifold of dimension n , it is well known that

$$\dim H_n(X) = 1.$$

and that

$$H_k(X) = 0, \text{ for any } k > n.$$

The generator $[\mu]$ of $H_n(X; \mathbb{Q})$, called the *class fundamental* of X verifies the following:

$$[\mu] \frown [\sigma] \in H_{n-k}(X), \text{ for any } [\sigma] \in H^k(X).$$

We get the following linear application

$$\begin{aligned} D: H^k(X) &\longrightarrow H_{n-k}(X) \\ [\sigma] &\longmapsto D[\sigma] := [X] \frown [\sigma] \end{aligned} .$$

Theorem 1.3

Poincaré duality: If X is a closed and orientable manifold of dimension n , then the application

$$D: H^k(X; \mathbb{Q}) \longrightarrow H_{n-k}(X; \mathbb{Q}) \text{ is an isomorphism.}$$

In other words,

$$H^k(X) \cong H_{n-k}(X).$$

For further details on both homology and cohomology we suggest these standard references: [29] and [49].

5

Homotopy



Definition 1.17

Set $I: = [0, 1]$, and let X and Y be two given topological spaces. We call a homotopy from X to Y , any continuous map:

$$H: X \times I \longrightarrow Y.$$

Then two continuous maps $f, g: X \rightarrow Y$ are said to be homotopic, when there is a homotopy $H: X \times I \rightarrow Y$, such that

$$H(-, 0) = f, \quad H(-, 1) = g,$$

then we write

$$f \sim g,$$

which define an equivalence relation on continuous maps from X to Y .



Definition 1.18

Two given topological spaces X and Y , are said to be homotopic, or have the same homotopy type if and only if there exist two continuous maps $f: X \rightarrow Y$ and $g: Y \rightarrow X$ such that

$$f \circ g \sim \text{id}_Y, \quad g \circ f \sim \text{id}_X.$$

This leads to an equivalence relation on the category **Top** of topological spaces endowed with continuous maps.

Definition 1.19

An algebraic object $\text{obj}(X)$ associated to a topological space X , is defined to be a homotopical invariant when

$$\text{obj}(X) \cong \text{obj}(Y),$$

for any $X \sim Y$.



Theorem 1.4

The following algebraic objects are homotopically invariant

1. The homology: $X \sim Y \implies H_*(X) \cong H_*(Y)$;
2. Betti numbers: $X \sim Y \implies \beta_k(X) = \beta_k(Y)$;
3. Homological and cohomological dimensions: $X \sim Y \implies \dim H_*(X) = \dim H_*(Y)$ and $\dim H^*(X) = \dim H^*(Y)$;
4. Euler-Poincaré invariant: $X \sim Y \implies \chi_c(X) = \chi_c(Y)$.

Definition 1.20

Let X be a path-connected topological space, and n a fixed integer.

The n -homotopy group of X is defined to be

$$\pi_n(X) := \text{map}(\mathbb{S}^n, X) / \sim,$$

where \mathbb{S}^n denoted the unit sphere of \mathbb{R}^{n+1} , and $\text{map}(\mathbb{S}^n, X) / \sim$ the quotient set of continuous maps $\gamma: \mathbb{S}^n \rightarrow X$, up to homotopy.



Remark 1.2

With respect to the denotations above, it is worth pointing out the following:

- The homotopy groups $\pi_n(X)$ are all abelian, for $n \geq 2$;

- $\pi_0(X)$ is nothing other than the set of the path components of X ;
- $\pi_1(X)$ called the fundamental group of X , describes, when loops in X are homotopic. $\text{card}(\pi_1(X))$ interprets the numbers of "holes" in X .
In particular, if X is simply connected, then $\pi_i(X) = \{0\}$.



Definition 1.21

Let X and Y be two topological spaces, then any continuous map $f: X \rightarrow Y$ can be extended naturally to the homotopy groups, by setting:

$$\begin{aligned} \pi_n(f): \pi_n(X) &\longrightarrow \pi_n(Y) \\ [\gamma] &\longmapsto [f \circ \gamma] \end{aligned}$$

f is said to be a *weak homotopy equivalence*, when all $\pi_n(f)$ are isomorphisms.

Hence X and Y are said to have the same *weak homotopy type*.



Definition 1.22

Let X and Y be two given topological spaces, A a fixed subset of X and $f: A \rightarrow Y$ a continuous map.

We call an *attachment* of X with respect to f , the quotient set $X \cup_f Y$ obtained while identifying any element $x \in A$ with its image $f(x) \in Y$.

More precisely,

$$X \cup_f Y := (X \amalg Y) / x \sim f(x),$$

where $X \amalg Y$ denotes the disjoint geometrical sum of X and Y .

Vocabulary: Let n be a fixed integer.

- We call n -cell, generally denoted e^n , any topological space that is homeomorphic to the open disk $D(0, 1)$ of \mathbb{R}^n ;
- We call n -skeleton, generally denoted $X^{(n)}$, any topological space that can be obtained by the attachment of $X^{(n-1)}$ to a finite number of n -cells;

- By convention, 0-skeletons, $X^{(0)}$, are any discrete collections of points.



Definition 1.23

We call a CW-complex, any topological space of the form $X = \bigcup X^{(n)}$ obtained by successive attachment of cells, and that verifies the following:

- **Closure-finite:** The boundary of each cell is equal to a disjoint union of a finite number of cells of smaller dimensions;
- **Weak topology:** If X is endowed with the weak topology, then a subset A of X is open, if and only if $A \cap X^n$ is open for any $n \in \mathbb{N}$.

The category of CW-complexes turns out to be a good category to work in homotopy, as the following results illustrate:



Definition 1.24

A continuous map $f: X \rightarrow Y$ between two CW-complexes is called a *cellular map*, if it injects any n -skeleton of X into a n -skeleton of Y .

More precisely, if $f(X^{(n)}) \subset Y^{(n)}$, for any $n \in \mathbb{N}$.



Theorem 1.5

Cellular Approximation Theorem: Any continuous map between two CW-complexes is homotopic to a cellular map.



Theorem 1.6

Whitehead Theorem: Any weak homotopy equivalence between two CW-complexes is a homotopy equivalence.

Definition 1.25

We call a cellular model of a topological space X , any CW-complex that has the same weak homotopy type of X .

Theorem 1.7

Cellular Model Theorem: Any topological space has a cellular model, unique up to homotopy.

For further details on homotopy, we suggest this standard reference: [69].

Chapter 2

Rational Homotopy Theory

1

Introduction

An element of a group is said to be without torsion when its order is infinite. The group itself is said to be without torsion, or free of torsion, when its unity is the unique element with torsion. If we tensor a group G , then we obtain a \mathbb{Q} -vector space $G \otimes \mathbb{Q}$, which is an abelian group without torsion. Basically, the aim of the rational homotopy theory, founded in the 1960s by D. Quillen [52] and D. Sullivan [61], is to study the rational homotopy type of a topological space by ignoring the torsion of its homotopy groups.



Definition 2.1

A topological space is said to be rational, when all its homotopy groups are \mathbb{Q} -vector spaces.



Theorem 2.1

If X is a simply connected CW-complex, then there exists a rational simply connected CW-complex, $X_{\mathbb{Q}}$, such that

$$\pi_n(X) \otimes \mathbb{Q} \cong \pi_n(X_{\mathbb{Q}}) \text{ as } \mathbb{Q}\text{-vector spaces.}$$

$X_{\mathbb{Q}}$ is called the *rationalization* of X , and its homotopy type is called the homotopy type of X .

In fact, the birth of rational homotopy went back a little further to 1950, when H. Hopf conjectured the following:



Conjecture 1

The homotopy type of any topological space can be modelled by a \mathbb{Q} -graded Lie algebra.

P. Serre was the first to study the non-torsion of the homotopy and homology groups. In 1953, he resolved the Hopf conjecture in this particular case:



Theorem 2.2

The rational weak homotopy type of any finite product of spheres of odd dimensions can be modelled by a semi-simple, compact and connected Lie group.

In 1967, D. Quillen resolved completely the Hopf conjecture in a rational context. He stated that:



Theorem 2.3

The rational homotopy type of any simply connected and pointed topological space can be modelled by a Lie group.



Theorem 2.4

The rational weak homotopy equivalence of any finite product of spheres of odd dimensions can be modelled by a semi-simple, compact and connected Lie group.

Quillen's work represented a crucial step toward the development of the rational homotopy theory, by justifying theoretically the reliability of the algebraic model as an efficient tool to determine the rational homotopy type of a topological space. However, his work suffered from a major flaw: the calculations were generally difficult or even impossible.

In the early 1970s, D. Sullivan tackled this problem of calculations, and proposed a model dual to that of Quillen. Sullivan's model is a co-chain of commutative algebras, based on piecewise linear rational forms. When publishing his first results, Sullivan pointed to the possibility of applying his models to resolve some geometric problems, such as the study of non-abelian periods in a differential manifold.

He claims that:

Any reasonable geometric construction on a topological space can be reflected by another finite, algebraic, using minimal models.

2

Hilali Conjecture

We were interested especially in some open problems related to elliptic spaces: the topological spaces X , whose rational homotopy $\pi_*(X) \otimes \mathbb{Q}$, and rational homology $H_*(X; \mathbb{Q})$ are both of finite dimension. Around 2007, our research focused on the following open problem:



Conjecture 2

Hilali conjecture (Topological version), [32]: For any simply

connected elliptic space X , we have:

$$\dim H^*(X; \mathbb{Q}) \geq \dim (\pi_*(X) \otimes \mathbb{Q}).$$

One of the powerful tools we used from rational homotopy theory, was the Sullivan minimal model, which relates by a homotopy equivalence the category of simply connected topological spaces to that of commutative differential graded algebras. This allows topologists to transpose many of their topological problems in an algebraic version, as follows:



Theorem 2.5

Sullivan [61]: For any simply connected topological space X of finite type, i.e., $\dim H^k(X; \mathbb{Q}) < \infty$ for all $k > 0$, there exists a commutative differential graded algebra $(\Lambda V, d)$, called the *minimal Sullivan model* of X , which algebraically models the rational homotopy of X , in the sense that

$$\pi_n(X) \otimes \mathbb{Q} \cong V \text{ as vector spaces,}$$

and that

$$H_*(X; \mathbb{Q}) \cong H_*(\Lambda V, d) \text{ as algebras.}$$

That means that any simply-connected topological space X , can be replaced by a rational CW-complex $X_{\mathbb{Q}}$, without exchanging either the rational homotopy type, or the rational cohomology. In particular, we get:

$$\begin{aligned} \dim H_*(X; \mathbb{Q}) &= \dim H_*(\Lambda V, d); \\ \dim \pi_n(X) &= \dim V, \end{aligned}$$

and the



Conjecture 3

Hilali conjecture (Algebraic version), [32]: If $(\Lambda V, d)$ is a simply connected and elliptic model of Sullivan, then

$$\dim V \leq \dim H^*(\Lambda V, d).$$

Before our works, the conjecture holds uniquely for pure models ($\dim V^{\text{even}} = \dim V^{\text{odd}}$), [32]:



Theorem 2.6

If $(\Lambda V, d)$ is a simply connected and elliptic pure model of Sullivan, then

$$\dim V \leq \dim H^*(\Lambda V, d).$$

From 2008, we proved the following:



Theorem 2.1

Hilali & M. (2008), [36]: The Hilali conjecture holds for H-spaces.

Let us recall that H-spaces are topological spaces whose Sullivan models are of the form $(\Lambda V, d)$. Topological groups are particular examples of H-spaces.



Theorem 2.2

Hilali & M. (2008), [36]: The Hilali conjecture holds for simply connected and elliptic topological spaces X , such that

$$\text{fd}(X) \leq 10,$$

where $\text{fd}(X) := \max\{k \in \mathbb{N}, \dim H^k(X; \mathbb{Q}) \neq 0\}$.



Theorem 2.3

Hilali & M. (2008), [36]: The Hilali conjecture holds for simply connected and hyper-elliptic minimal Sullivan models, under some restrictive conditions.

Let us recall that a minimal Sullivan model $(\Lambda V, d)$ is called hyper-elliptic whenever it satisfies the following:

$$dV^{\text{even}} = 0 \text{ and } dV^{\text{odd}} \subset \Lambda V^{\text{even}} \otimes \Lambda V^{\text{odd}}.$$

Pure models are particular examples of hyper-elliptic under our restrictive conditions.



Theorem 2.4

Hilali & M. (2008), [36]: The Hilali conjecture holds for symplectic manifolds, for cosymplectic manifolds, and for nilmanifolds.

We especially show that for such manifolds, the inequality in the Hilali conjecture is strict.



Theorem 2.5

Hilali & M. (2008), [37]: The Hilali conjecture holds for simply connected and elliptic formal topological spaces.

Formal spaces are topological spaces whose minimal Sullivan models $(\Lambda V, d)$ verify the following:

$$V = U \oplus W, \text{ with } dV = 0, \text{ and } dW \text{ is a regular sequence in } \Lambda U.$$

Examples of formal spaces include spheres, H-spaces, symmetric spaces, and compact Kähler manifolds.



Theorem 2.6

Hilali & M. (2008), [37]: The Hilali conjecture holds for simply connected and elliptic minimal Sullivan models $(\Lambda V, d)$ whose differential is homogeneous of length at least 3, i.e. $dV \subset \Lambda^{\geq 3} V$.

Around 2014, we investigated the case of coformal spaces, those for whom the differential of the Sullivan model is purely quadratic, i.e., $dV \subset \Lambda^2 V$. We especially prove the following:



Theorem 2.7

Elkrafi, Hilali & M. (2015), [13]: The Hilali conjecture holds for any coformal space X whose rational homotopy Lie algebra \mathbb{L} is of nilpotency 1 or 2.

We also proposed some research directions to resolve completely the coformal case by induction on the nilpotency degree of the associated homotopy Lie algebra. In fact, resolving completely the coformal case would be a decisive step towards the definitive resolution of the Hilali conjecture, since the case when the differential is homogeneous of length at least 3 was already resolved. The Hilali conjecture now belongs to the rational homotopy theory folkloric open problems, and it gave rise to a lot of research interests and is now stated in many interesting cases, such as:

- Hyper elliptic Sullivan models, see [4];
- Two stages Sullivan models, i.e. when $V = U \oplus W$ with $dU = 0$ and $dW \subset \Lambda^{\geq 2}U$, see [1].

We also investigate the Hilali conjecture for configuration spaces of manifolds. Let us recall that



Definition 2.2

If M is given a manifold and k a fixed non null integer, then

$$F(M, k) = \{(x_1, x_2, \dots, x_k) \in M^k, x_i \neq x_j \text{ for } i \neq j\}$$

denotes the space of all ordered configurations of k distinct points in M .

Our main result states that



Theorem 2.8

Hilali, M. and Yamoul (2015), [39]: If M is a closed and simply connected manifold, then $F(M, k)$ verifies the Hilali conjecture provided that $F(M, k)$ is elliptic.

We also proved the following



Theorem 2.9

Hilali, M. and Yamoul (2015), [39]: If M is rationally elliptic, and $X = M - \{pt\}$ has a non-trivial rational homotopy group in dimension > 1 , then $F(X, 2)$ and $F(M, k)$ for $k > 2$, are rationally

- hyperbolic.



Theorem 2.10

Hilali, M. and Yamoul (2015), [39]: If M is a simply connected manifold of dimension at least 3, and has at least two linearly independent elements in its rational cohomology, then $F(M, 3)$ and in general $F(M, k), k \geq 3$ is rationally hyperbolic.

where a topological space is said to be hyperbolic, whenever its homology is of infinite dimension

3

Halperin Conjecture

Around 2016 we were especially interested in:



Conjecture 4

Halperin conjecture [30]: For any elliptic space X , we have:

$$\dim H^*(X; \mathbb{Q}) \geq 2^{\text{rk}_0(X)},$$

where $\text{rk}_0(X)$, called the toral rank, is defined to be the maximum, or the infinity, of integers n such that the toral \mathbb{T}^n acts almost freely on X .

We firstly make the connection possible between this conjecture and that of Hilali, thanks to the following results:

Let χ_c and χ_π be the cohomological and homotopic Euler-Poincaré characteristics of X , respectively defined by:

$$\begin{aligned} \chi_c &= \sum_{k \geq 0} (-1)^k \dim H^k(X; \mathbb{Q}); \\ \chi_\pi &= \sum_{k \geq 0} (-1)^k \dim \pi_n(X) \otimes \mathbb{Q}. \end{aligned}$$

Then, following the last theorem, we get

$$\begin{aligned}\chi_c &= \dim H^{\text{even}}(X; \mathbb{Q}) - \dim H^{\text{odd}}(X; \mathbb{Q}); \\ \chi_\pi &= \dim V^{\text{even}} - \dim V^{\text{odd}}.\end{aligned}$$



Theorem 2.7

Halperin, [31]: If X is a simply connected and elliptic topological space, then

$$\chi_c \geq 0 \text{ and } \chi_\pi \leq 0.$$

Moreover,

$$\chi_c > 0 \iff \chi_\pi = 0.$$

In other words,

$$\dim H^{\text{even}}(X; \mathbb{Q}) \geq \dim H^{\text{odd}}(X; \mathbb{Q}),$$

and

$$\dim V^{\text{even}} \leq \dim V^{\text{odd}}.$$

Moreover,

$$\dim H^{\text{even}}(X; \mathbb{Q}) > \dim H^{\text{odd}}(X; \mathbb{Q}) \iff \dim V^{\text{even}} = \dim V^{\text{odd}}.$$



Theorem 2.8

Allday-Halperin, [2]: If X is a simply-connected and finite CW-complex then

$$\text{rk}_0(X) \leq -\chi_\pi.$$

The preceding theorems combined with the definitions of χ_c and χ_π allow us to set:

$$\begin{aligned}\dim V^{\text{pair}} &= n \\ \dim V^{\text{impair}} &= n + p \quad \text{with } p \geq 0 \\ \dim V &= 2n + p \\ \chi_\pi &= -p \\ \text{rk}_0(X) &= p - \varepsilon \quad \text{where } \varepsilon \geq 0\end{aligned}$$

The Hilali conjecture becomes

$$\dim H^*(\Lambda V, d) \geq 2n + p.$$

That of Halperin is now equivalent to

$$\dim H^*(\Lambda V, d) \geq 2^{p-\varepsilon}.$$



Remark 2.1

The promised connection is written as follows:

$$\begin{aligned} \text{Hilali conjecture} + (2n \geq 2^{p-\varepsilon} - p) &\implies \text{Toral rank conjecture} \\ \text{Toral rank conjecture} + (2n \leq 2^{p-\varepsilon} - p) &\implies \text{Hilali conjecture} \end{aligned}$$

We show that



Theorem 2.11

El Krafi, Hilali and M., (2016), [13]: The toral rank conjecture holds for any manifold of dimension less than 16, and whose rational toral rank is equal to 4.

4

Theriault Conjecture

Around 2015 we were interested in the rational homotopy version of the following open question asked by S. Theriault: Given a topological space X , what may one say about the nilpotency of $\text{aut}_1(X)$ when the cocategory of its classifying space $\text{Baut}_1(X)$ is finite? Here $\text{aut}_1(X)$ denotes the path component of the identity map in the set of self homotopy equivalences of X . More precisely, we proved that

$$\text{Hnil}_{\mathbb{Q}}(\text{aut}_1(X)) \leq \text{cocat}_{\mathbb{Q}}(\text{Baut}_1(X)),$$

when X is a simply connected CW-complex of finite type and that the equality holds when $\text{Baut}_1(X)$ is coformal. Many intersections with other popular open questions were stated.

In fact, many different definitions of the cocategory were known:

- rational version: $\text{cocat}_{\mathbb{Q}}$, defined in [58];
- Hovey version: Hcocat , defined in [34];
- inductive version: indcocat , defined in [27];
- Whitehead approach version: wcocat defined in [33].

We know that

$$\text{wcocat}(X) \leq \text{indcocat}(X) \leq \text{Hcocat}(X) \leq \text{cocat}_{\mathbb{Q}}(X).$$

We focused on the rational version of the cocategory given by Sbaï in terms of Quillen models in the following sense:



Definition 2.3

The *minimal Quillen model* is dual to the Sullivan minimal model and involves free differential graded Lie algebras (DGLA) (\mathbb{L}_W, ∂) , in opposite of CDGA. Here W is a graded vector space W , and \mathbb{L}_W is equipped with a decomposable differential (i.e., $\partial : \mathbb{L}_W \rightarrow \mathbb{L}_W^{\geq 2}$), where \mathbb{L}_W^k designates the set of brackets of length k .

Quillen showed in [52], that any simply connected and rational CW-complex of finite type X , admits a minimal Quillen model (\mathbb{L}_W, ∂) , unique up to isomorphism, which encodes the rational homotopy type as follows:

$$\begin{aligned} H_*(\mathbb{L}_W, d) &\cong \pi_{*+1}(X) \otimes \mathbb{Q} \\ W &\cong \check{H}_{*+1}(X; \mathbb{Q}) \end{aligned} .$$

In particular, $\partial \mathbb{L}_W \subset \mathbb{L}_W^2$ when X is formal, while $\mathbb{L}_W \simeq \pi_{*+1}(X) \otimes \mathbb{Q}$ in the coformal case.

Sbaï defined in [58] the rational cocategory of X , denoted throughout this book by $\text{cocat}_{\mathbb{Q}}(X)$, to be the smallest integer (or infinite) such that the projection

$$(\mathbb{L}_W, \partial) \longrightarrow (\mathbb{L}_W / \mathbb{L}_W^{\geq n+1}, \partial)$$

admits a retract. In particular we have:

- $\text{cocat}_{\mathbb{Q}}(X) = 0$ if and only if X is contractible;

- $\text{cocat}_{\mathbb{Q}}(S^{2n+1}) = 1$ and $\text{cocat}_{\mathbb{Q}}(S^{2n}) = 2$.

On the other hand, given X , a topological space,

- $\text{aut}(X)$ denotes the set of its self homotopy equivalences, that are maps $f : X \rightarrow X$ that admit a homotopy inverse;
- $\text{aut}_1(X)$ denotes the identity path component.

S. Theriault asked the following:



Conjecture 5

Theriault's open question: Is it true that $\text{Hnil}(\text{aut}_1(X))$ is finite whenever $\text{cocat}(\text{Baut}_1(X))$ is?

Here, $\text{Hnil}(\text{aut}_1(X))$ denotes the *homotopical nilpotency* of $\text{aut}_1(X)$, viewed as a connected grouplike space. That is the least integer n such that the $(n+1)$ -th commutator c_{n+1} is nullhomotopic. Note that the iterated commutators $c_n: G^n \rightarrow G$ are inductively defined, using the homotopy inverse, as follows: c_1 is the identity, $c_2(a, b) = aba^{-1}b^{-1}$ and $c_n = c_2 \circ (c_{n-1}, c_1)$. We answered positively to this open question in a rational homotopy theory setting. More precisely we proved that:



Theorem 2.12

El Krafi and M. (2017), [15]: Let X be a simply connected CW-complex of finite type. If $\text{cocat}_{\mathbb{Q}}(\text{Baut}_1(X))$ is finite, then $\text{Hnil}_{\mathbb{Q}}(\text{aut}_1(X))$ is also. Moreover, we have

$$\text{Hnil}_{\mathbb{Q}}(\text{aut}_1(X)) \leq \text{cocat}_{\mathbb{Q}}(\text{Baut}_1(X)).$$

and that



Theorem 2.13

El Krafi and M. (2017), [15]: Let X be a simply connected CW-complex of finite type, such that $\text{Baut}_1(X)$ is coformal. If $\text{cocat}_{\mathbb{Q}}(\text{Baut}_1(X))$ is finite, then $\text{Hnil}_{\mathbb{Q}}(\text{aut}_1(X))$ is also. More-

over, we have

$$\text{Hnil}_{\mathbb{Q}}(\text{aut}_1(X)) = \text{cocat}_{\mathbb{Q}}(\text{Baut}_1(X)).$$

The formal case was discussed in



Theorem 2.14

El Krafi and M. (2017), [15]: Let X be a simply connected CW-complex of finite type, such that $\text{Baut}_1(X)$ is formal. If $\text{cocat}_{\mathbb{Q}}(\text{Baut}_1(X))$ is finite, then $\text{Hnil}_{\mathbb{Q}}(\text{aut}_1(X))$ is also. Moreover, we have

$$\text{Hnil}_{\mathbb{Q}}(\text{aut}_1(X)) \leq 2.$$

In addition of solving completely Theriault's open question in a rational context, our theorems fit nicely with other well known open problems: the formality or coformality of $\text{Baut}_1(X)$. Indeed, when $\text{Baut}_1(X)$ is of finite rational cocategory, our results induce that $\text{Hnil}_{\mathbb{Q}}(\text{aut}_1(X)) \neq \text{cocat}_{\mathbb{Q}}(\text{Baut}_1(X))$ is an obstruction of the coformality of $\text{Baut}_1(X)$, while the inequality $\text{Hnil}_{\mathbb{Q}}(\text{aut}_1(X)) > 2$ is an obstruction of the formality of $\text{Baut}_1(X)$. Note also that H-spaces are formal, and that still opened a more general question, if $\text{Baut}_1(X)$ is a rational H-space? We proved that:



Theorem 2.15

El Krafi and M. (2017), [15]: If G is a topological group such that $\text{Baut}_1(G)$ is a rational H-space with a finite rational cocategory, then

$$\text{Hnil}(G) \leq 2.$$

In particular, $\text{Baut}_1(G)$ may be H-space only if $\text{Hnil}(G) \leq 2$ (i.e. G is homotopically trivial or abelian or its inner automorphism group is abelian).

Rational homotopy type classification

Since 2011, we have been interested in the folkloric problem to classify the rational homotopy type. Problem which gave rise to many research works (see [5],[43], [59], [64], [65], [66]). Our approach is to assemble a catalogue in higher dimensions which will lead to seeing some pattern. We were able to classify, following their rational homotopy type, all simply connected and elliptic topological spaces whose cohomological dimension is less than 9. Details of our classification are summarised in the following tables:



Theorem 2.16

Hilali, Lamane and M. (2012), [35]: If X is a simply connected and elliptic space with cohomological dimension equal to 8 and whose homotopical invariant χ_π is non zero, then its rational homotopy type is given by:

Rational homotopy type	Condition
$\mathbb{S}^{2k+1} \times \mathbb{S}^{2k+1} \times \mathbb{S}^{2k+1}$	$\text{fd}(X) = 3(2k + 1)$
$\mathbb{S}^n \times \mathbb{S}^n \times \mathbb{S}^{2n}$	$\text{fd}(X) = 4n$, with n is odd
$(\mathbb{S}^n \times \mathbb{S}^n \times \mathbb{S}^{2n}) \# \mathbb{S}_{(2)}^{2n}$	$\text{fd}(X) = 4n$, with n is even
$\mathbb{S}^{2k+1} \times \mathbb{S}^{2k+1} \times \mathbb{S}^{2(k+p)}$	$\text{fd}(X) = 2(2k + 1) + 2(k + p)$
$\mathbb{S}^{2n} \otimes (\mathbb{S}^n \times \mathbb{S}^{2n}) \times \mathbb{S}^{2(n+p)+1}$	$\text{fd}(X) = 4n + 2(n + p) + 1$
$\mathbb{S}^{2n} \times \mathbb{S}^{2n} \times \mathbb{S}^{2(n+p)+1}$	$\text{fd}(X) = 4n + 2(n + p) + 1$
$\mathbb{S}^{2n} \times \mathbb{S}^{2(n+p)+1} \times \mathbb{S}^{2(n+p)+1}$	
$\mathbb{S}^{2n} \times \mathbb{S}^k \times \mathbb{S}^k$	$k \geq 2n + 2$
$\mathbb{S}^{2n} \times \mathbb{S}^{2k+1} \times \mathbb{S}^{2(n+k)+1}$	
$\mathbb{S}^{2n} \otimes (\mathbb{S}^{2k+1} \times \mathbb{S}^{2(n+k)+1})$	
$\mathbb{S}_{(3)}^n \otimes \mathbb{S}^{2k+1}$	
$\mathbb{S}^{2k+1} \otimes \mathbb{S}^{2n+1} \otimes \mathbb{S}^{2p+1}$	
E	E : the total space of the fiber with $\mathbb{S}^{2k+1} \otimes \mathbb{S}^{2n+1}$ as base space
$\mathbb{S}^{2n+1} \times Y_a$	$a \in \mathbb{Q}^*$



Theorem 2.17

Hilali, M. and Yamoul (2016), [40]: If X is a simply connected and elliptic space whose cohomological dimension is less than 8, then its rational homotopy type is given by:

$\dim H^*(X; \mathbb{Q})$	Rational homotopy type
1	*
2	\mathbb{S}^n
3	$\mathbb{S}_{(2)}^n$
4	$\mathbb{S}^n \times \mathbb{S}^m$ $\mathbb{S}_{(3)}^n$ Y_λ with $H^*(Y_\lambda; \mathbb{Q}) = \mathbb{Q}[a, b]/(ab, a^2 - \lambda b^2)$
5	$\mathbb{S}_{(4)}^n$ $\mathbb{S}_{(3)}^n \# \mathbb{S}_{(2)}^m$
6 and $\chi_\pi = 0$	$\mathbb{S}_{(5)}^n$ $\mathbb{S}^n \times \mathbb{S}_{(2)}^m$ P_λ with $H^*(P_\lambda; \mathbb{Q}) = \mathbb{Q}[a, b]/(ab, a^2 - \lambda b^4)$ Q_λ with $H^*(Q_\lambda; \mathbb{Q}) = \mathbb{Q}[a, b]/(b^2 + ab + \lambda a^2)$ R_λ with $H^*(R_\lambda; \mathbb{Q}) = \mathbb{Q}[a, b]/(a^3, b^2 + \lambda a^2)$
6 and $\chi_\pi \neq 0$	$\mathbb{S}^n \times \mathbb{S}_{(2)}^m$ $T_{n,m}$, the total space of the fibration $\mathbb{S}^{n+m-1} \rightarrow T_{n,m} \rightarrow \mathbb{S}^n \times \mathbb{S}^m$
7	$\mathbb{S}_{(6)}^n$ $\mathbb{S}_{(2)}^n \# \mathbb{S}_{(5)}^m$ $\mathbb{S}_{(3)}^n \# \mathbb{S}_{(4)}^m$ R with $H^*(R; \mathbb{Q}) = \mathbb{Q}[a, b]/(a^2 b, a^3 - b^2)$
8 and $\chi_\pi = 0$	$\mathbb{S}_{(7)}^n$ $\mathbb{S}_{(4)}^n \times \mathbb{S}_{(2)}^m$ $\mathbb{S}_{(4)}^n \# \mathbb{S}_{(4)}^n$ $\mathbb{S}_{(5)}^n \# \mathbb{S}_{(3)}^m$ $\mathbb{S}_{(2)}^n \times \mathbb{S}_{(2)}^m \times \mathbb{S}_{(2)}^k$ $P_{a,b,c}$ with $H^*(P_{a,b,c}; \mathbb{Q}) = \mathbb{Q}[a, b, c]/(a^2 - abc, b^2 - abc, c^2 - abc)$



Theorem 2.18

Hilali, M. and Tarik (2015), [38]: If X is a simply connected and elliptic space such that $\dim H^*(X; \mathbb{Q}) = 9$, then its rational homotopy type is given by the following table

$H^*(X; \mathbb{Q}) \cong$	$(\Lambda V, d) \cong$
$\mathbb{Q}[a]/(a^9)$	$(\Lambda(a, x), d)$ with $da = 0, dx = a^9$
$\mathbb{Q}[a, b]/(ab, a^7 - b^2)$	$(\Lambda(a, b, x, y), d)$ with $da = db = 0$ $dx = ab, dy = a^7 - b^2$
$\mathbb{Q}[a, b]/(ab, a^6 - b^3)$	$(\Lambda(a, b, x, y), d)$ with $da = db = 0$ $dx = ab, dy = a^6 - b^3$
$\mathbb{Q}[a, b]/(ab, a^5 - b^4)$	$(\Lambda(a, b, x, y), d)$ with $da = db = 0$ $dx = ab, dy = a^5 - b^4$
$\mathbb{Q}[a, b]/(a^3, b^3)$	$(\Lambda(a, b, x, y), d)$ with $da = db = 0$ $dx = a^3, dy = b^3$
$\mathbb{Q}[a, b]/(a^3 + ka^2b, b^3 + k'ab^2)$	$(\Lambda(a, b, x, y), d)$ with $da = db = 0$ $dx = a^3 + ka^2b$ $dy = b^3 + k'ab^2$
$\mathbb{Q}[a, b]/(a^2b, a^5 - b^2)$	$(\Lambda(a, b, x, y), d)$ with $da = db = 0$ $dx = a^2b, dy = a^5 - b^2$
$\mathbb{Q}[a, b]/(a^3 - ab, ka^6 + k'b^3)$	$(\Lambda(a, b, x, y), d)$ with $da = db = 0$ $dx = a^3 - ab$ $dy = ka^6 + k'b^3$
$\mathbb{Q}[a, b]/(a^3b, a^3 - b^2)$	$(\Lambda(a, b, x, y), d)$ with $da = db = 0$ $dx = a^3 - b^2, dy = a^3b$

Chapter 3

Topological Robotics

1

Introduction

Around 2012, we switched to applied algebraic topology, especially to its application in robotics. The topological study of the *robot motion planning algorithms* emerged in 2003-2004 with the works of M. Farber (see [17], [18]). In fact, motivated by the topological study of the motion planning algorithms using tools from algebraic topology, Michael Farber considered a path connected topological space X , and equipped its path space PX with the compact open topology. He viewed any motion planning algorithm of any mechanical robot that moves on the configuration space X to be an:

- Input: a pair (A, B) of two given points in the configuration space X ;
- Output: a continuous path from A to B and hence a continuous section

$$\begin{aligned} s: X \times X &\longrightarrow PX \\ (A, B) &\longmapsto s(A, B) \end{aligned}$$

of the canonical projection

$$\begin{aligned} \pi: PX &\longrightarrow X \times X \\ \gamma &\longmapsto (\gamma(0), \gamma(1)) \end{aligned} .$$

The path-connectedness of X ensures the existence of such section. Its continuity, which ensures the robot stability while moving through X , is equivalent to the contractibility of X , (i.e. X is homotopic to a point). Roughly speaking, the continuity of motion planners means that close initial-final pairs (A, B) and (A', B') produce close motions $s(A, B)$ and $s(A', B')$. In other words it interprets the stability of the motion, when the configuration space X is contractible.

2

Topology of motion planning algorithms

We were especially interested to learn more about the topology of the non empty set of the continuous motion planning algorithms, denoted here $\mathcal{M}(X)$, where X is a path-connected and contractible topological space. We firstly topologized $\mathcal{M}(X)$ with the open-compact topology as a subset of $\text{map}(X \times X, PX)$. Our first main result states that



Theorem 3.1

Derfoufi and M. (2015), [24]: If X is a path-connected and contractible CW-complex, then $\mathcal{M}(X)$ is also contractible.

However $\mathcal{M}(X)$ is contractible, i.e., homotopically trivial, it is not necessarily topologically poor. We focused later on the study of its topological properties by considering the special case, when X is a normed vector space. In fact, when X is a normed vector space, the open-compact topology on PX coincides with that of the uniform convergence and this allows us to study the stability of a robot motion using norms. We especially prove that



Theorem 3.2

Derfoufi and M. (2015), [24]: If X is a normed vector space, then $\mathcal{M}(X)$ is a regular space.

Let us recall, that



Definition 3.1

A topological space X is said to be regular, when for any non empty closed set K and any point $x \notin K$, there exists a neighbourhood U of x and a neighbourhood V of K that are disjoint.

Concisely speaking, it is always possible to separate x and K with disjoint neighbourhoods, when $x \notin K$.

Our second purpose was to approximate motion planning algorithms on X by piecewise affine ones. This is very useful, in the sense that although we know enough about the existence of motion planning algorithms, we know less how to describe and determine it explicitly, hence one can appeal to some discretization methods to explicit some motion planning algorithms. More precisely, we proved that:



Theorem 3.3

Derfoufi and M. (2015), [24]: If X is a normed vector space, and K is a compact of $X \times X$, then $\mathcal{M}_{K, PX}^{\text{Aff}}$ is dense in $\mathcal{M}_{K, PX}$.

Here $\mathcal{M}_{K, PX}^{\text{Aff}}$ denotes the local piecewise affine motion planning algorithms on any compact subset K of $X \times X$, where



Definition 3.2

A motion planning algorithm s on X is called piecewise affine if and only if for any pair of points $A, B \in X$, there exists a subdivision

$t_0 = 0 < t_1 < \dots < t_{n-1} < t_n = 1$ of $[0, 1]$ such that


$$s(A, B)(t) = a_i t + b_i, \text{ on each } [t_i, t_{i+1}].$$

3

Loop topological complexity

As seen here above, when the configuration space X is contractible, the robot motion is stable. In the opposite case, and in order to mea-

sure the complexity of this stability, M. Farber defined the homotopy invariant $TC(X)$, called *topological complexity*, to be:

 **Definition 3.3**

$TC(X)$ is the minimum among the normalized cardinalities of all open coverings $(U_i)_{0 \leq i \leq k}$ of $X \times X$, over each of which

$$\begin{aligned} \text{ev}: PX &\longrightarrow X \times X \\ \gamma &\longmapsto (\gamma(0), \gamma(1)) \end{aligned} .$$

has a local continuous section $s_i: U_i \longrightarrow PX$, i.e.,

$$\text{ev} \circ s_i = \text{id}_{U_i} .$$

It was well known, that have:

- $TC(X) = 0$ if and only if $X \sim *$, from [17];
- $TC(X) = 1$ if and only if $X \sim \mathbb{S}^{2n+1}$, from [28];
- $TC(\mathbb{S}^{2n}) = 2$, from [17].

In his founding paper [17], M. Farber was not interested in the return motion. He made up for this some years after and focused with M. Grant on the symmetric case (i.e., when the robot's going and coming motions are the same). They defined the notion of *symmetric topological complexity*, denoted $TC^S(-)$, and showed that

$$TC(X) \leq TC^S(X) \quad \text{see [19)].}$$

We were tempted to waive this restriction on the return motion and let the robot free to take any arbitrary way to come back to its departure point, as in the case of the motion of a drone, or an unmanned air-plane, or a guided TV camera. The famous NP-complete problem of vehicle routing with pick-up and delivery can also be studied throughout this angle.

That was our first inspiration to define and study topologically and homotopically the concept of *loop motion planning algorithm* (LMPA for short).



Definition 3.4

A LMPA over X , is any continuous section $s: X \times X \rightarrow LX$ of the loop bi-evaluation

$$\begin{aligned} ev^{LP}: LX &\rightarrow X \times X \\ \gamma &\mapsto (\gamma(0), \gamma(\frac{1}{2})) \end{aligned} .$$

Here, the *free loop space*, $LX := \{\gamma : X^{S^1} \rightarrow X \text{ continuous}\}$ is endowed with open-compact topology, the input is a pair of points (A=departure, B=target), while the output should suggest to the robot a target by requiring a come-back to the departure point. We firstly proved that:



Theorem 3.4

Derfoufi and M. (2015), [25]: If X is a path-connected topological space, then LMPAs on X exist if and only if X is contractible.

Following Farber's spirit we define the *loop topological complexity* of X , denoted here $TC^{LP}(X)$, to be:



Definition 3.5

$TC^{LP}(X)$ is minimum among the normalized cardinalities of all open coverings $(U_i)_{0 \leq i \leq k}$ of $X \times X$, over each of which ev^{LP} has a local continuous section $s_i: U_i \rightarrow LX$ (i.e., $ev^{LP} \circ s_i = id_{U_i}$).

In particular, we proved that:



Theorem 3.5

Derfoufi and M. (2015), [25]: If X is a path-connected topological space, then $TC^{LP}(X)$ is a homotopical invariant, meaning:

$$X \sim Y \Rightarrow TC^{LP}(X) = TC^{LP}(Y).$$

and that



Theorem 3.6

Derfoufi and M. (2015), [25]: If X is a path-connected topological space, then

$$\text{TC}^{\text{LP}}(X) = \text{TC}(X).$$

In addition to investigating a neglected specific robot motion, the loop motion one; our approach yields to many applications and connections with other results or well known open problems. The most awesome, but not the least one, is that our loop TC generalizes both the classical notion (introduced by M. Farber in [17]) and the symmetric one (introduced by M. Farber and M. Grant in [19]). Moreover, whilst the symmetry of a going and coming robot motion increases the complexity navigation, our requirement that the return is free does not.

It is useful to note also the deep intersection between the loop TC and the monoidal TC (denoted $\text{TC}^M(-)$ and introduced by Iwase-Sakai in [41]): the two focus on the special case when the initial position of a robot motion coincides with the terminal one. Our theorem may be viewed as a possible research direction supporting the famous Iwase-Sakai conjecture (see [42]) about coincidence of the ordinary topological complexity TC and the monoidal one TC^M .

Finally, we raised an open question: Though $\mathcal{M}_{\text{LP}}(X)$ is homotopically trivial, algebraically it is not. The natural questions are: What can one do or interpret (in terms of robotics) with this loop motion product? What structure does it induce?

The answer to this question leads us to a new exciting research work as will be described in the next section.

4

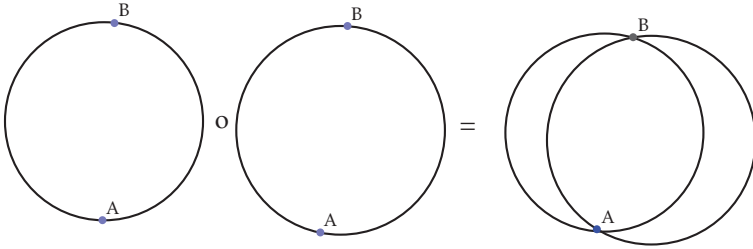
String Topological Robotics

As mentioned above, we were tempted to study the topological, homotopical or algebraic behaviour of the set of LMPA, denoted here $\mathcal{M}_{\text{LP}}(X)$. Firstly, we noted that $\mathcal{M}_{\text{LP}}(X)$ as a map space can be topologized with the induced open compact topology. Secondly, we have seen that $\mathcal{M}_{\text{LP}}(X)$ is non empty if and only if X is contractible. In this case, $\mathcal{M}_{\text{LP}}(X)$ is also contractible.

Our first inspiration came from the natural concatenation of loops. Therefore we firstly define a kind of concatenation on loop motion planner, that we called the *loop motion product*. For any given LMPAs s_1 and s_2 we put:

$$\begin{aligned} \mu(s_1, s_2)(A, B)(t) &= s_1(A, B)(t) && \text{if } 0 \leq t \leq \frac{1}{2} \\ &= s_1(A, B)(3t - 1) && \text{if } \frac{1}{2} \leq t \leq \frac{2}{3} \\ &= s_2(A, B)(3t - 2) && \text{if } \frac{2}{3} \leq t \leq 1 \end{aligned}$$

As illustrated here below, two LMPAs are composable if and only if they have two common base points.



This was our first inspiration to investigate homologically the behaviour of motion planners while [20], wherein a natural homomorphism of commutative graded algebras

$$\Gamma: H_*(\text{Sect}(q)) \longrightarrow \mathbb{H}_*(X^{S^1}): = H_{*+n}(X^{S^1})$$

is well defined, where $\text{Sect}(q)$ denotes the sections of the free loop

space fibration

$$q: \begin{array}{ccc} X^{S^1} & \longrightarrow & X \\ \gamma & \longmapsto & \gamma(0) \end{array} .$$

As a key idea for their proof, Y. Félix and J. C. Thomas pointed out that the composition of loops makes $\text{Sect}(q)$ into a monoid with multiplication μ defined by

$$\mu(s_1, s_2)(x)(t) = \begin{cases} s_1(A)(2t) & t \leq \frac{1}{2} \\ s_2(A)(2t-1) & t \geq \frac{1}{2} \end{cases} \quad \sigma, \tau \in \text{Sect}(q), t \in [0, 1], x \in X$$

While reading Félix-Thomas approach in [21] to generalize Chas-Sullivan *string topology* into a broad rational homotopy theoretical setting, we get the inspiration to generalize Chas-Sullivan string theory into a broad topological robotics setting.

A primary motivation of the string theory was a remarkable problem posed by Sullivan in [60]: find a class of spaces with singularities for which the signature of manifolds extends as an invariant cobordism. The intersection homology groups provide a partial answer for complex varieties. For their purpose, Chas-Sullivan assumed manifolds to be closed and orientable. They started by extending the concept of intersection product to $LX := X^{S^1}$. Chas-Sullivan's approach consisted to:

- consider two families of based loops: $\Sigma \in C_i(LX; \mathbb{Z})$ an i -chain of loops in X , and $\Theta \in C_j(LX; \mathbb{Z})$ a j -chain of loops in X ;
- intersect transversally in X the associative marked i -chain $\Sigma(0) \in C_i(X; \mathbb{Z})$ and j -chain $\Theta(0) \in C_j(X; \mathbb{Z})$;
- obtain an $(i+j-n)$ -chain $\Sigma(0) \cdot \Theta(0)$ in X , along which the marked points of Σ coincide with that of Θ ;
- create in LX a new $(i+j-n)$ -chain $\Sigma \bullet \Theta$, by concatenating at each point of $\Sigma \cdot \Theta$, loops that go around the loops of Σ and then around the loops of Θ .

In fact, string topology works as follows. One has to :

- consider the evaluation map at time $t = 0$ defined by

$$ev_0: \begin{array}{ccc} C_i(LX; \mathbb{Z}) & \longrightarrow & C_i(X; \mathbb{Z}) \\ \Sigma & \longmapsto & \Sigma(-)(0): \delta \in \Delta^i \mapsto \Sigma(\delta)(0) \end{array} .$$

It links i -simplices in LX to that in X . Here Δ^i denotes the i -simplicial standard and 0 is the base point of $S^1 = \mathbb{R}/\mathbb{Z}$;

- consider some simplices $\Sigma: \Delta^i \rightarrow LX$ and $\Theta: \Delta^j \rightarrow LX$, such that $ev_0(\Sigma)$ and $ev_0(\Theta)$ intersect transversally in X .
- compute the intersection product $\Sigma(-)(0) \cdot \Theta(-)(0)$ at each point $(\delta, \delta') \in \Delta^i \times \Delta^j$ such that $\Sigma(\delta)(0) = \Theta(\delta')(0)$;
- perform the composition of the loops $\Sigma(\delta)$ and $\Theta(\delta')$ to obtain a *loop product*, the $(i + j - n)$ -simplex $\Sigma \bullet \Theta: \Delta^{i+j-n} \rightarrow LX$;
- define the *loop homology* by $\mathbb{H}_*(LX) := H_{*+n}(LX; \mathbb{Z})$.

The loop product (see [10]) passes to the homology and defines the *string product*

$$\mathbb{H}_i(X) \otimes \mathbb{H}_j(X) \xrightarrow{\bullet} \mathbb{H}_{i+j}(X)$$

which endows $\mathbb{H}_*(X)$ with a structure of an associative and commutative graded algebra (see [10]). Finally, they defined a loop bracket $\{, \}$ which passes to loop homology and induces on $\mathbb{H}_*(X)$ a structure of Gerstenhaber algebra (i.e., the bracket is a bi-derivation of \bullet and satisfies the Jacobi identity). They also defined an operator Δ which endows $\mathbb{H}_*(X)$ with a structure of Batalin-Vilkovisky algebra.

Now it is time to present our string topological robotics theory claiming to link both topological robotics and string topology. For this purpose, we consider G a compact Lie group which operates transitively on a path connected n -manifold, X . (contractible or not, compact or not, orientable or not). In other words, the mechanical system presents a symmetry with respect to a given compact Lie group.

Our first step was to set

$$LX \times_{X/G} LX := \{(\gamma, \tau) \in LX \times LX : G \cdot \gamma(1/2) = G \cdot \tau(0)\}.$$

and

$$ev^{LP}: LX \times_{X/G} LX \longrightarrow X \times X$$

$$(\gamma, \tau) \longmapsto (\gamma(0), \tau(1/2))$$

$LX \times_{X/G} LX$ can be viewed as a $G \times G$ -space with the obvious multiplication

$$(g_1, g_2)(\gamma, \tau) = (g_1 \cdot \gamma, g_2 \cdot \tau)$$

and $ev^{LP}: LX \times_{X/G} LX \rightarrow X \times X$ as a $G \times G$ -fibration.

Definition 3.6

We call a *G-loop motion planner* (*G-LMP* for short), any $G \times G$ -homotopic section of the loop evaluation ev^{LP} . That is any $G \times G$ -map

$$\begin{aligned} s: X \times X &\longrightarrow LX \times_{X/G} LX \\ (x, y) &\longmapsto (\gamma, \tau) \end{aligned}$$

such $ev^{\text{LP}} \circ s$ is $G \times G$ -homotopic to $\text{id}_{X \times X}$.

In other words, for any given pair $(x, y) \in X^2$, there exists a pair of loops $(\gamma, \tau) \in LX \times LX$ such that $\gamma(0) = x, \tau(1/2) = y$ with $G.x = G.y$ and that where the transitivity of the action interferes. Here, global sections are not asked to be continuous and X is not required to be contractible. Therefore

$$\mathcal{M}^{\text{LP}}(X) := \text{Sect}(ev^{\text{LP}})$$

is not necessarily contractible, and therefore its homology is not trivial.

Secondly, inspired by Laudenbach's works (see [45]), we defined the bi-evaluation

$$\begin{aligned} ev_{0,1/2}: \mathcal{M}^{\text{LP}}(X) &\longrightarrow X^2 \\ s &\longmapsto (s(-, -)(0), s(-, -)(1/2)) \end{aligned}$$

to link $\Sigma : \Delta^i \longrightarrow \mathcal{M}^{\text{LP}}(X)$ as an i -simplex of $\mathcal{M}^{\text{LP}}(X)$ to $\sigma := ev_{0,1/2}(\Sigma) : \Delta^i \longrightarrow X^2$ as an i -simplex of X^2 . Their faces are also linked thanks to the relation

$$F(ev_{0,1/2}\Sigma) = ev_{0,1/2}(F\Sigma)$$

Definition 3.7

Let us now equip X^2 with a chart \mathcal{A} . A simplex Σ of $\mathcal{M}^{\text{LP}}(X)$ is said to be *small* when there exists $U(\Sigma) \in \mathcal{A}$ (chosen once for all) such that $\sigma(\Delta^i) \subset U(\Sigma)$.

Thus, to a j -simplex $\Theta: \Delta^j \rightarrow \mathcal{M}^{\text{LP}}(X)$ of $\mathcal{M}^{\text{LP}}(X)$ we associated $\theta := ev_{0,1/2}(\Theta)$ as a j -simplex in X , and we call the bi-simplex $\Sigma \times \Theta: \Delta^i \times \Delta^j \rightarrow \mathcal{M}^{\text{LP}}(X) \times \mathcal{M}^{\text{LP}}(X)$ *small* when both Σ and Θ are small. $\Sigma \times \Theta$ is said to be *transverse* when $\sigma \times \theta$ and all its faces are transverse in X^4 to the diagonal map

$$\Delta_{X^2}: \quad X^2 \quad \longrightarrow \quad X^4 \quad . \\ (x, y) \quad \longmapsto \quad (x, y, x, y)$$

Under such conditions,

$$W := (\Delta_{X^2} \circ (\sigma \times \theta))^{-1}(X^4)$$

is an orientable sub-manifold of $\Delta^i \times \Delta^j$ with corners and of dimension $i + j - 2n$.

Let ev be used for short to denote $ev_{0,1/2}$. To any pair $(\delta_1, \delta_2) \in W$ we associated the pair

$$(s_1, s_2) := (\Sigma \times \Theta)(\delta_1, \delta_2) \in \mathcal{M}^{\text{LP}}(X) \times \mathcal{M}^{\text{LP}}(X).$$

The following commutative diagram outline the situation

$$\begin{array}{ccc} (\delta_1, \delta_2) \in W \subset \Delta^i \times \Delta^j & \xrightarrow{\Sigma \times \Theta} & (s_1, s_2) \in \mathcal{M}^{\text{LP}}(X) \times \mathcal{M}^{\text{LP}}(X) \\ & \searrow \sigma \times \theta & \downarrow ev \times ev \\ & & \Delta_{X^2} \subset X^2 \times X^2 \end{array}$$

In particular,

$$ev \times ev(s_1, s_2) = (s_1(-, -)(0), s_1(-, -)(1/2), s_2(-, -)(0), s_2(-, -)(1/2))$$

as an element of Δ_{X^2} is of the form (x, y, x, y) . Thus s_1 and s_2 are composable since they have two commons base points, namely $x = s_1(-, -)(0) = s_2(-, -)(0)$ and $y = s_1(-, -)(1/2) = s_2(-, -)(1/2)$ and the precedent diagram can be performed to get this diagram

$$\begin{array}{ccccc} & & \Sigma, \Theta : \text{intersection LMP product} & & \\ & & \text{-----} & & \\ W \simeq \Delta^{i+j-2n} & \xrightarrow{\Sigma \times \Theta} & \mathcal{M}^{\text{LP}}(X) \times \mathcal{M}^{\text{LP}}(X) & \xrightarrow{\mu} & \mathcal{M}^{\text{LP}}(X) \\ & \searrow \sigma \times \theta & \downarrow ev \times ev & & \\ & & \Delta_{X^2} \simeq X^2 & & \end{array}$$

This allowed us to define the *intersection product* as follows

Definition 3.8

Let $\Sigma : \Delta^i \rightarrow \mathcal{M}^{\text{LP}}(X)$ and $\Theta : \Delta^j \rightarrow \mathcal{M}^{\text{LP}}(X)$ two simplices in $\mathcal{M}^{\text{LP}}(X)$ of respective dimensions i and j . Their intersection LMP product $\Sigma \cdot \Theta : \Delta^{i+j-2n} \rightarrow \mathcal{M}^{\text{LP}}(X)$ is defined by

$$\Sigma \cdot \Theta := \mu \circ (\Sigma \times \Theta)|_{W}.$$

It can be extended naturally and linearly at the level of small and transverse bi-chains.

Let $C_*(\mathcal{M}^{\text{LP}}(X))$ denote the chain complex generated by the small simplices, and ε_k be the sign of the Jacobian of the coordinates change $U(F_k \Sigma) \rightarrow U(\Sigma)$. The next step consisted to define the homology of LMPs

Definition 3.9

Let $\partial : C_i(\mathcal{M}^{\text{LP}}(X); \mathbb{Z}) \rightarrow C_{i-1}(\mathcal{M}^{\text{LP}}(X); \mathbb{Z})$ the *boundary operator* defined by

$$\partial \Sigma := \sum_{k=0}^i \varepsilon_k (-1)^k F_k \Sigma.$$

Then we put

$$H_*(\mathcal{M}^{\text{LP}}(X); \mathbb{Z}) := H_*(C_*(\mathcal{M}^{\text{LP}}(X), \partial)).$$

After that, we extended, at the level of the homology $H_*(\mathcal{M}^{\text{LP}}(X); \mathbb{Z})$, the intersection LMP product to a *string LMP product* by setting

$$\begin{aligned} \bullet \quad H_i(\mathcal{M}^{\text{LP}}(X); \mathbb{Z}) \times H_j(\mathcal{M}^{\text{LP}}(X); \mathbb{Z}) &\longrightarrow H_{i+j-2n}(\mathcal{M}^{\text{LP}}(X); \mathbb{Z}) . \\ ([\Sigma], [\Theta]) &\longmapsto [\Sigma] \bullet [\Theta] := [\Sigma \cdot \Theta] \end{aligned}$$

Finally, we proved that this string LMP product is well defined, in the sense that any given pair of homological classes $([\Sigma], [\Theta])$ can be represented by a small and transverse bi-simplex and that the homological class $[\Sigma \cdot \Theta]$ does not depend on the choice of this bi-simplex. Indeed, we defined the following:

Definition 3.10

A boundary preserving homotopy of a given chain $\Theta = \sum_k n_k \Theta_k \in C_*(\mathcal{M}^{\text{LP}}(X); \mathbb{Z})$ is a homotopy parameter family $\Theta^t = \sum_k n_k \Theta_k^t$, with $\Theta^0 = \Theta$ and such that if Θ_k^t and Θ_p^t have a common face at time $t = 0$, then it is also at any time t .

and proved that

Theorem 3.7

Derfoufi and M. (2016), [26]: For any bi-chain $\Sigma \times \Theta$, there exists a boundary preserving homotopy Θ^t of Θ such that $\Sigma \times \Theta^1$ is small and transverse.

Theorem 3.8

Derfoufi and M. (2016), [26]: The string LMP product is associative and commutative up to sign. More precisely,

$$[\Sigma] \bullet [\Theta] = (-1)^{|\Sigma| \cdot |\Theta|} [\Theta] \bullet [\Sigma].$$

Finally, by applying the regrading $\mathbb{H}_* := H_{*+2n}$, we got the following :

Theorem 3.9

Derfoufi and M. (2016), [26]: $\mathbb{H}_*(\mathcal{M}^{\text{LP}}(X); \bullet)$ have a structure of graded commutative and associative ring.

In [47], we realize our aim, that to endow $(\mathbb{H}_*(\mathcal{M}^{\text{LP}}(X)), \bullet)$ with structures of Gerstenhaber and Batalin-Vilkovisky algebras, we firstly adapt our notations to that of Chas-Sullivan in order to adapt the geometric "proof" of Chas and Sullivan to our "robotic" setting. Hence $\Sigma: \Delta^i \rightarrow \mathcal{M}^{\text{LP}}(M)$ and $\Theta: \Delta^j \rightarrow \mathcal{M}^{\text{LP}}(M)$ will be replaced respectively by $x: K_x \rightarrow \mathcal{M}^{\text{LP}}(M)$ and $y: K_y \rightarrow \mathcal{M}^{\text{LP}}(M)$. Therefore for any $k_x \in K_x$, one have

$$\begin{aligned} x(k_x): \quad M \times M &\longrightarrow LM \times_G LM \\ (m_0, m_1) &\longmapsto x(k_x)(m_0, m_1) \end{aligned}$$

with

$$\begin{aligned} x(k_x)(m_0, m_1)(0) &= m_0 \\ x(k_x)(m_0, m_1)(1/2) &= m_1 \end{aligned}$$

If $\bar{x} \times \bar{y}: K_x \times K_y \times [0, 1] \rightarrow M^2 \times M^2$ is transverse to both Δ_{M^2} and all its faces, then the loop operator on LMP, $0, *$ emerges on

$$K_{x*y} := (\bar{x} \times \bar{y})^{-1}(\Delta_{M^2}) = K_x \times_{M^2} K_y \times [0, 1]$$

by putting

$$x * y(k_x, k_y, s)(-, -)(t) := \begin{cases} y(k_y)(-, -)(2t) & 0 \leq t \leq \frac{s}{2} \\ x(k_x)(-, -)(1 - 2t + s) & \frac{s}{2} \leq t \leq \frac{s+1}{2} \\ y(k_y)(-, -)(2t - 1) & \frac{s+1}{2} \leq t \leq 1 \end{cases}$$

Moreover, and as in the Chas-Sullivan context, $x * y$ follows y from $y(k_y)(-, -)(0)$ to $y(k_y)(-, -)(s)$, then from $y(k_y)(-, -)(s)$ to $y(k_y)(-, -)(1)$ after traversing x . For $s = 0$, we find $x \bullet y$, while $s = 1$ induces $y \bullet x$. Keeping this useful remark in mind, we claim that at the level of the homology, we have.



Theorem 3.10

M. (2020), [49]:

$$x \bullet y = (-1)^{|x||y|} y \bullet x.$$

and more precisely



Theorem 3.11

M. (2020), [49]: $\mathbb{H}_*(\mathcal{M}^{\text{LP}}(M))$ is an associative and commutative graded algebra.

Before going through defining the LMP bracket, we prove that



Theorem 3.12

M. (2020), [49]:

$$x * (y \bullet z) \simeq (x * y) \bullet z + (-1)^{(|x|+1)|y|} y \bullet (x * z);$$

$$\bullet (x \bullet y) * z \simeq x \bullet (y * z) + (-1)^{(|z|+1)|y|} (x * z) \bullet y.$$

And set

 **Definition 3.11**

M. (2020), [49]:

$$\{x, y\} := x * y - (-1)^{(|x|+1)(|y|+1)} y * x.$$

Finally, we get

 **Theorem 3.13**

[?] M. (2020), [49]: $\mathbb{H}_*(\mathcal{M}^{\text{LP}}(M), \bullet, \{, \})$ is Gerstenhaber algebra. Meaning that

- $\mathbb{H}_*(\mathcal{M}^{\text{LP}}(M), \bullet)$ is an associative and commutative graded algebra;
- $\{, \}$ is Lie bracket of degree 1;
- $\{x, y \bullet z\} = \{x, y\} \bullet z + (-1)^{(|x|+1)|y|} y \bullet \{x, z\}.$

The natural way to get a Batalin-Vilkovisky algebra structure is to use the circle action on LMPs and define the operator

$$\Delta x(k_x, s)(t) := x(k_x)(t + s).$$

Chapter 4

Topological Data Analysis

1

Introduction

From 2016, we switched to another exciting area of research in the applied algebraic topology. *Topological Data Analysis* (TDA for short) is an emerging trend in exploratory data analysis and data mining. It has known a growing interest and some notable successes (such as the identification of a new type of breast cancer, or the classification of NBA players, or the prediction of the future USA president) in recent years. Indeed, with the explosion in the amount and variety of available data, identifying, extracting and exploiting their underlying structure has become a problem of fundamental importance. Many such data come in the form of point clouds, sitting in potentially high-dimensional spaces, yet concentrated around low-dimensional geometric structures that need to be uncovered.

The non-trivial topology of these structures is challenging for classical exploration techniques such as dimensionality reduction. The goal is therefore to develop novel methods that can reliably capture geometric or topological information (connectivity, loops, holes, curvature, etc) from the data without the need for an explicit mapping to lower-dimensional space. Persistent homology is the main tool of the TDA, it consists to represent any shape under a barcode. As the saying goes, "every data have a shape, and any shape have a meaning". Thus the key idea of TDA is to represent a data as a shape

(a point cloud for example), and the issue its barcode (the meaning of the data).

In the TDA community we agree, without formalizing it, that H. Edelsbrunner is the founder of this theory. Indeed, the fast algorithm described in his leader paper [14] triggered the explosion of interest we currently observe because its availability as software facilitates its application to a broad collection of problems and datasets.

We agree also that the G. Carlsson research works (see [8]), and that the software platform and applications offered by its machine intelligence software company Ayasdi, are the precursors of the current popularity of TDA both in the scientific and industrial communities. For example, one widely reported top five globally important bank was that to build models required for the annual Comprehensive Capital Analysis and Review (CCAR) process took 1,800 person-months with traditional manual big data analytic and machine learning tools, but took 6 person-months with Ayasdi. Now, Ayasdi, founded in 2008, is considered as "A Big Data Start-Up With a Long History"¹, and recently announced a new 55 million USD of funding, led by Kleiner Perkins Caufield & Byers (KPCB), and joined by existing investors, Institutional Venture Partners (IVP), Khosla Ventures, FLOODGATE, Citi Ventures, and other new investors, Center View Capital Technology and Draper Nexus.

2

Persistent homology

Persistent homology, as a topological data analysis tool, is a young and quickly-developing research area at the intersection of mathematics, statistics, and computer science. It seeks to use topology to discern structure in a complex data by studying its shape.² Topology takes on two main tasks: the measurement of shape and the representation of shape. Both tasks are meaningful in the context of large, complex, and high-dimensional data-sets. They allow measurement of shape related properties within the data, such as the presence of holes.

¹The New York Times. January 16, 2013.

²G. Carlson: Any data has a shape and any shape has a meaning

Given a point cloud, we want to use homology to describe data, but our data is a point cloud and homology operates on simplicial complexes. The first step is to associate to any points cloud a Čech complex.

Definition 4.1

Given a cloud of points $X = (x_i)_i$ and a number $\varepsilon > 0$, the associated Čech complex $C(\varepsilon)$ is the simplicial complex whose p -simplicies are the $[x_0, \dots, x_p]$, whenever the balls $B(x_i, \varepsilon/2)$ have a common point.

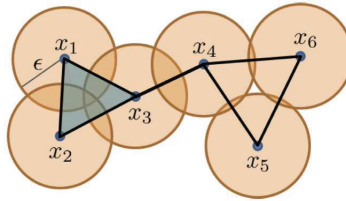


Figure 4.1: An example of a points cloud (left) and the corresponding Čech complex.

While ε is growing, other Čech complexes will appear, and this yields to a filtration of complexes

$$\emptyset = \mathcal{K}^0 \subseteq \mathcal{K}^1 \subseteq \dots \subseteq \mathcal{K}^m = \mathcal{K}.$$

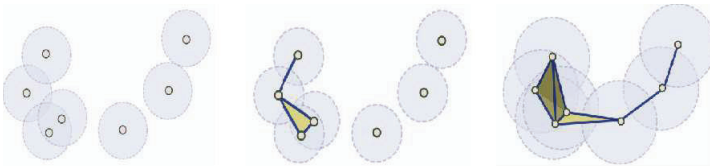


Figure 4.2: Example of filtered Čech complex.

The associated homology of that kind of chain of complexes, is what we call the persistent homology of the initial cloud of points

$X = (a_i)_j$. The idea of persistent homology is to look for features that persist for some range of parameter values. Typically a feature, such as a hole, will initially not be observed, then will appear, and after a range of values of the parameter it will disappear again. The resulting persistent Betti numbers are usually given as barcodes, and represent how the homology changes through the filtration.

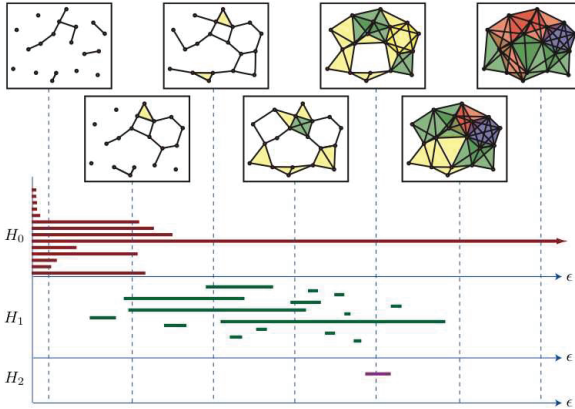


Figure 4.3: From points cloud to barcodes.

The beginning of a barcode can be thought of as a birth time of a persistent homology class and its end as the death time. The significance of a homological feature is given by the length of the corresponding barcode. It is a way to encode the persistent homology of a data set in the form of a parametric version of a Betti number and represents each persistent generator with a horizontal line beginning at the first filtration level where it appears, and ending at the filtration level where it disappears.

A persistent diagram is another equivalent way to visualize the evolution of the topological features in the filtration, by summarizing the filtration as two dimensional point sets with multiplicities. A point (x, y) with multiplicity m represents m features that all appear for the first time at scale x and disappear at scale y . Features appear before they disappear, as the points lie above the diagonal $x = y$. The difference $y - x$ is called the persistent of a feature. A class of homology that appears at times i and disappears in another value j will be represented by the point of coordinates (i, j) . The persistent of a class will be the real value of $j - i$, this diagram is called persistent diagram

because it will encode the persistent of the homology groups of the simplex. An interesting case of persistent diagrams is that associated to \mathbb{R} -valued functions $f : X \rightarrow \mathbb{R}$, where the filtration is given by the sub level sets $X_\varepsilon := f^{-1}(-\infty, \varepsilon]$.

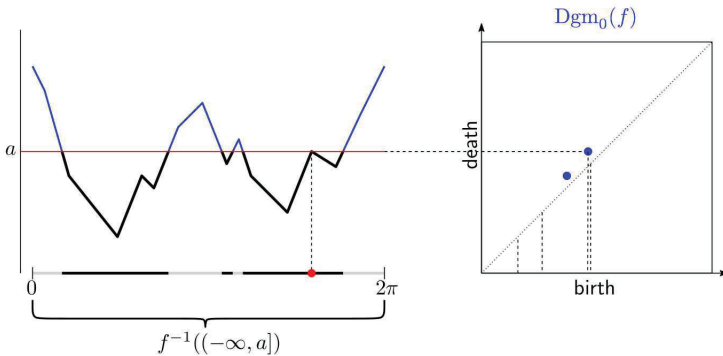


Figure 4.4: Example of persistent diagram.

One way to compare how two persistent diagrams are closed or not, is the Bottleneck distance used to calculate the distance between two persistence diagrams D_1 and D_2 by setting

$$d_B(D_1, D_2) := \inf_{\mu} \sup_{x \in D_1} \|x - \mu(x)\|_{\infty},$$

where $\mu: D_1 \rightarrow D_2$ range all the bijections from D_1 to D_2 .

The fundamental result that has allowed the scientific recognition that persistent homology enjoys now is the *stability theorem* which states that a small perturbation in the input filtration leads to a small perturbation of its persistence diagram.



Stability theorem 4.1

Let $f, g: X \rightarrow \mathbb{R}$ two tame functions, then

$$d_B(\text{Dgm}(f), \text{Dgm}(g)) \leq \|f - g\|_{\infty}.$$

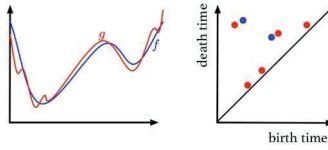


Figure 4.5: Bottleneck distance is 1-Lipschitz function.

3

Images Recognition

One of the exciting application areas of mathematics we investigated was the recognition of objects in digital images. It has received the attention of many researchers in order to evaluate and improve the performance of descriptors, especially that of the shape descriptor. Indeed, a huge amount of images are produced and analysed in different domains such as biology, industry, astronomy, medicine and security. These images contain some interesting objects that have to be recognized, classified and then identified. To represent an image or a part of it and describe the pertinent information, we use the features extracted there-from. These extracted features are represented in different ways (vector, signature, barcode, ...). This representation is called a *shape descriptor*. The shape descriptors are a powerful tool used in a wide spectrum of computer vision and image processing tasks such as object matching, classification, recognition and identification.

It is useful to note that there exists a huge variety of object recognition approaches, but the general concept remains the same: An object recognition system uses training data sets containing images with known and labelled objects and extracts different types of information (colors, edges, shapes and so on) based on the chosen algorithm. The first step of a recognition system is to detect interest locations (objects) in the images and describe them. Once the descriptors are computed, they are compared to the objects presented in an image to recognize and identify them.

The shape descriptor relies on two types: The global features and the local ones. In the global one, the image is represented by one multidimensional feature vector, describing the information in the

whole image. On the other hand, local features allow detection of interest regions in an image and represent them as n vectors where each one describes a certain feature, like color, texture, shape or orientation. It is well known that local features are very successful, powerful and faster than global ones [BS]. This is due to the lack of accuracy for global features which generally can not distinguish the foreground from background of an image.

In [50], we considered the persistent homology as an algebraic tool measuring the topological features of shapes. To digital images, we associated cubical complexes instead of triangulation because it significantly reduces the size of complexes. We implement this algebraic characterization by an algorithm that represents any digital image as bare codes in the form of finite union of intervals. The benefits of this algorithm are not only the shape description, but also the shape comparison. Indeed, by using the Bottleneck distance of barcodes, the algorithm allows us to answer how close or far two shapes are. So, we developed a shape descriptor, based on persistent homology ideas. It is an algorithm, whose input is a digital image, and that issues some barcodes as a signature. The strength of our algorithm is that it combines the two classic approaches: the global one by involving all the pixels, and the local one by associating to each pixel 8 new neighbours thanks to the *Low Star Process*.

More precisely, our algorithm aims to represent the objects of an image (classes) as barcodes to get a shape signature (descriptor). This descriptor will be an efficient tool to recognize an object and identify it, this will be satisfied when we build a knowledge database that contains the objects of our interest with their barcodes and their label (identification). The output of the algorithm will be compared to all the objects present in the database until we find the most similar barcode.

For our purpose, we opted for cubical persistent homology as an efficient application of persistent homology in domains where the data is naturally given in a cubical form, as in the case of digital images. By avoiding triangulation of the data, we significantly reduce the size of the complex. The approach is to use n -cubes $[0, 1]^n$ instead of n -simplicies, the remainder (like boundary operator or boundary matrix) still roughly speaking the same.

Simplicial complexes are called *cubical complexes*, and the associ-

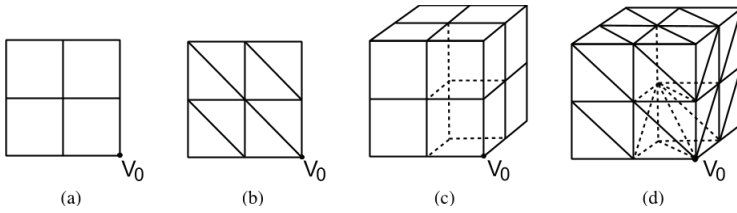


Figure 4.6: Cubical complex triangulation vs. simplicial complex triangulations.

ated persistent homology is called *cubical persistent homology*. In this new context, the non-null pixels play the point cloud. The cubical complex is kindly built as follows: To any pixel $B(i, j)$ (considered as 0-cube and colored in yellow), we associate 8 neighbours (four 1-cubes are colored in blue and four 2-cubes are colored in red).

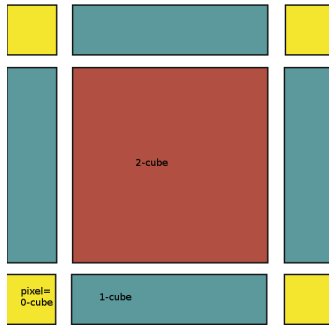


Figure 4.7: Cubical complex: The first step.

This representation of cubical complexes from images permit us to have an idea about the relationship between cells by reading their coordinates. For each pixel, we can store the necessary information in 3×3 array. The coordinates of any cell gives immediately its dimension:

- it is an 0-cube when its coordinates are (even,even);
- it is a 1-cube when its coordinates are (even,odd) or (odd,even);

- it is a 2-cube when its coordinates are (odd, odd).

Moreover, the benefit of this is that we can track down the past coordinates of any pixel by dividing the new ones by two.

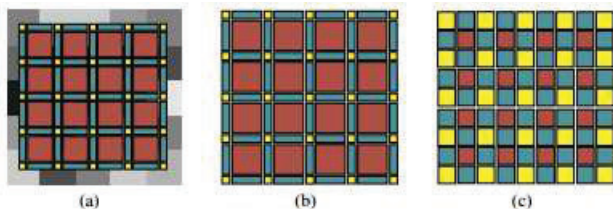


Figure 4.8: Cubical complex built over a gray-scale 2D image with 4x4 pixels.

It is worth pointing out, that if (i, j) are the coordinates of a pixel in the original binary matrix, those in the cubical complex should be $(2i, 2j)$. This is another strong point to count in favour of our algorithm; that to switch smoothly between the initial and the final coordinates by dividing or multiplying by 2. Thus we define a function "neighbours", whose aim is to associate to each pixel $B[i, j]$ its 8 neighbours $C[2i + \varepsilon, 2j + \varepsilon']$, where $\varepsilon, \varepsilon' \in \{-1, 0, 1\}$, with some excluded values, especially when the pixel is on the border. For example, $\varepsilon \neq -1$, whenever the pixel locates in west border. Our function (see Algorithm 1) takes into account this technical but useful detail.

Once the cubical complex was built as $(2I - 1) \times (2J - 1)$ -matrix), we set the following Algorithm 2) to preserve in any pixel the same as that in the original matrix. We use the *low-star* rule, which states that any n -cube and all its faces should have the same values. We firstly start with the pixel of high value, and assign this value to all its neighbours. We move on to the next one and assign the not yet assigned neighbours and so on.

Algorithm 1 Function neighbours((x,y),X):(x1,y1).

Input: A matrix and the position of an element

Output: Position of the neighbours of the element

for $X - 1 < x1 < X + 2$ **do**

for $Y - 1 < y1 < Y + 2$ **do**

if $-1 < x < X, -1 < y < Y, X! = x2 || Y! = y2, 0 < x1 < X, 0 < y1 < X$ **then**

 return(x1,y1)

end if

end for

end for

Algorithm 2 Function BuildComplex(B)

Input: Matrix filled with the pixels from the original matrix

Output: Matrix representing the cubical complex

$lp, [], flag = -1$

List L: elements of the original matrix sorted in descending order

for $i \leftarrow 0$ to $len(L)$ **do**

$posMax \leftarrow PositionOfL[i]inB$

$Lneighbors \leftarrow neighbors(posMax[0], posMax[1], B)$

$Lp \leftarrow add(Lneighbors)$

$flag \leftarrow flag + 1$

for $k \leftarrow 0$ to $len(lp)$ **do**

for $p \leftarrow 0$ to $len(lp[k])$ **do**

if $b[Lp[k][p][0], Lp[k][p][1]] == 0$ **then**

$[Lp[k][p][0], Lp[k][p][1]] = neighbors[flag]$

end if

end for

end for

end for

Sometimes, some values are extremely huge, in this case we normalize it by re-applying the transformations

$$B[i, j] \leftarrow B[i, j] + \frac{i+I*j}{\alpha+I*j}$$

$$B[i, j] \leftarrow \frac{B[i, j]}{\max B[i, j]}$$

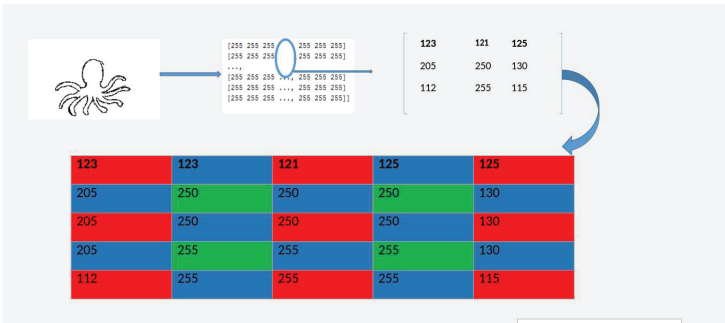


Figure 4.9: An example of a cubical complex from a digital image.

The next, crucial and important step consists of building the boundary matrix. We start by building a filtration in this natural ordering:

- $\mathcal{K}_0 = \emptyset$;
- $\mathcal{K}_1 =$ the 2-cube of high value and all its faces;
- $\mathcal{K}_2 =$ the next 2-cube and all its faces;
- Once all the 2-cubes are swept, we pass to the 1-cubes.

The boundary matrix should be a $N \times N$ -array, where N is the number of all different values that appear in the cubical complex. It should encode the evolution of the filtration here above. Thus in the 0-th stage all values will be null. In the first stage, we put boundary matrix(i,j)=1, once the j -th cube is a neighbour of the i -th cube, where the filtration indices are assigned from higher to lower

Algorithm 3 Function boundaryMatrix(Cubical complex C: matrix).

Input: Cubical matrix C (each cube has faces named B_j)

Output: Boundary matrix

```

for each cube  $C_i$  of K do
  Column  $\leftarrow$  filtration index of  $C_i$ 
  for each cube  $B_j$  in boundary of  $C_i$  do
    row  $\leftarrow$  filtration index of  $B_j$ 
    boundaryMatrix(row,column)  $\leftarrow$  1
  end for
end for

```

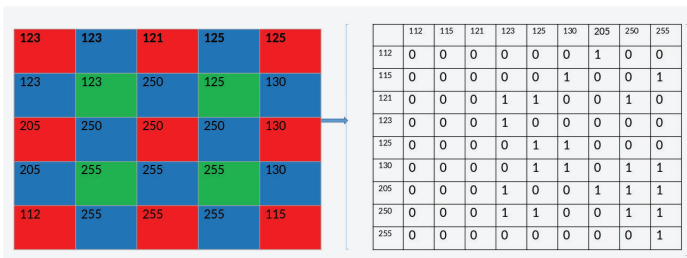


Figure 4.10: An example of a boundary matrix from a cubical complex.

The final step consists of reducing the boundary matrix following the [12] approach, where the Smith normal form of the boundary matrix is used to record the face relationship between simplices of dimension p and $p - 1$. Let $low(j)$ be the row number of the lowest non-zero entry in column j , where we set $low(j) = 0$ if the entire column is zero. A matrix is called *reduced* when each row has at most one entry that is the lowest 1 for a column. To reduce our boundary matrix, 0 proceed from left to right by using only column additions (see Algorithm 4).

Algorithm 4

Input: Boundary matrix
Output: Reduced boundary matrix
for $j \leftarrow 1$ to n **do**
 while $\exists j' < j$ with $low(j') \neq low(j)$ **do**
 add column j' to column j
 end while
end for

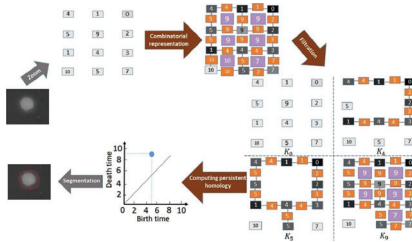


Figure 4.11: An example of a bare code from a digital image.

Fast and robust feature extraction is crucial for many computer vision applications. The performance of a shape descriptor or the efficiency of shape features is related to some essential properties, for example the location, the rotation and the scaling changing of the shape. Since our algorithm is based on the pixel coordinates, which it never loses thanks to its ability to track it at any time in the process, then such essential properties do not affect the extracted features which are still as robust as possible against noise.

Neuronal sciences

We focused sometimes on neuronal sciences, especially on the NASA experiences of Limoli and his team (see [54],[55], [56]) on the possible and significant damage in dendrites and spines in the neural networks of the Mars explorers that may be caused by cosmic radiation. Our key idea was to use the NASA images of some mice that were exposed for 12 weeks to cosmic radiation. We associate to their neural network bare codes that give us more information, than that given by the original experiences.

The neural networks are a neural arrangement, each neural is extended by a *dendrite* topped with thorns called *spines*. These spines play an important role in the communication between neurals.

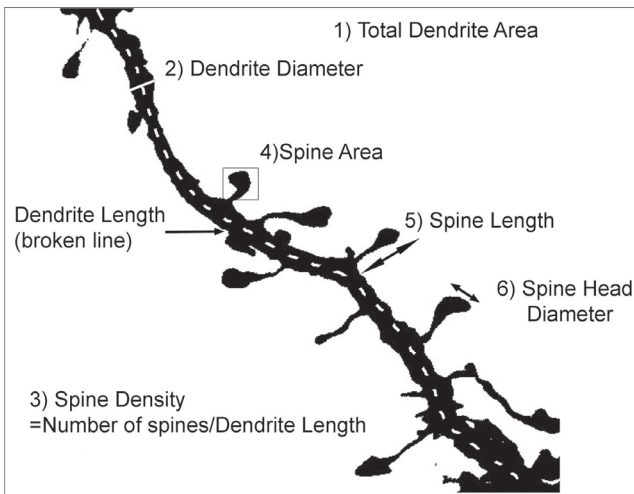


Figure 4.12: Structure of a typical dendrite.

Dendrites are the branches of neurons that receive signals from other neurons and pass the signals into the *cell body*. The *axon* is the part of a neuron that sends the signal. Axons that feel like a highly developed dendrite are long and thin. The axon carries an electrical signal from the cell body to the *synapse*: the structure that permits a neuron to pass an electrical or chemical signal to another neuron. Synapses

are essential to neuronal function: neurons are cells that are specialized to pass signals to individual target cells, and synapses are the means by which they do: A dendrite from one neuron and an axon from another neuron meet at a synapse.

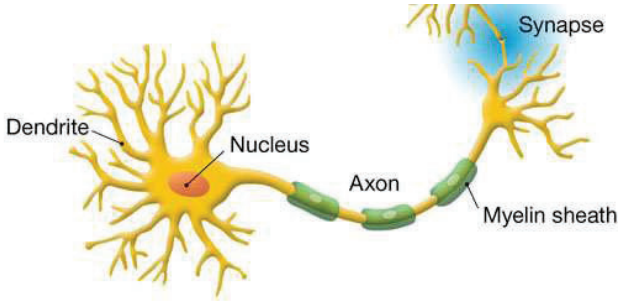


Figure 4.13: Communication process between two neurons.

Limoli and his team have to make an important breakthrough: to select the best candidates for a one-way trip to Mars. For this purpose, they took male mice to a particle accelerator at the NASA Space Radiation Laboratory to catapult oxygen and titanium ions down a 100-meter transport tunnel and into the restrained rodents' brains at roughly two-thirds the speed of light. Six weeks after this radiation exposure, they noticed distinct changes to the brains of the mice, notably inflammation that disrupted communication between the neurons. This breaking off of the neuronal structures known as dendrites, while the loss of the branch-like synapses are often associated with cognitive impairments and Alzheimer's disease. Going further, the NASA biologists did some behavioural experiments with the exposed mice to see how their neural tissue damage might affect their memory and learning abilities. Sure enough, the mice exhibited less curiosity and seemed more confused than mice who had not been exposed to space-like radiation. These symptoms are similar to the cognitive changes when cancer patients are undergoing radiation treatments.

Thus possible damage during a space mission may alter cognitive function, including detriments in short-term memory, reduced motor function, and behavioural changes, which may affect performance and human health. This radiation induces changes in synaptic plasticity underlying many neuro degenerative conditions that correlate to specific structural alterations in neurons that are believed to

be morphologic determinants of learning and memory. This cosmic radiation causes some cognitive dysfunction during the novel object recognition (NOR) task, the object in place (OiP) task or the temporal order (TO) task.

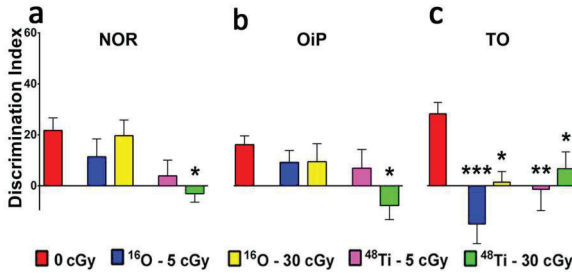


Figure 4.14: Cognitive deficits evaluated 12 weeks after cosmic radiation exposure.

The figure here below shows how irradiation significantly reduces the recognition memory, that it reduces the preference to explore an object found in a novel location and that it significantly impairs the memory by a reduced preference for the less recently explored object in the Temporal Order task (TO).

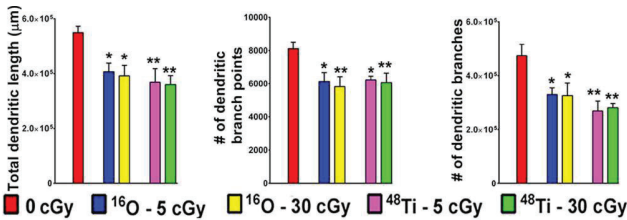


Figure 4.15: Reduced dendrite complexity of neurons after 12 weeks of cosmic radiation.

This quantification of the dendrite parameters, as bar charts, shows that the dendrite branching and length are significantly reduced 12 weeks after exposure to 5 or 30 cGy ^{48}Ti or ^{16}O or 30cGy ^{16}O particles.

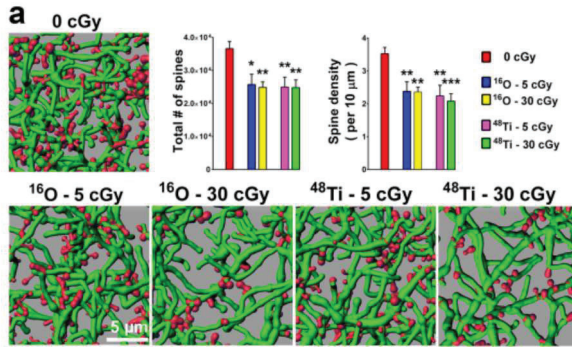
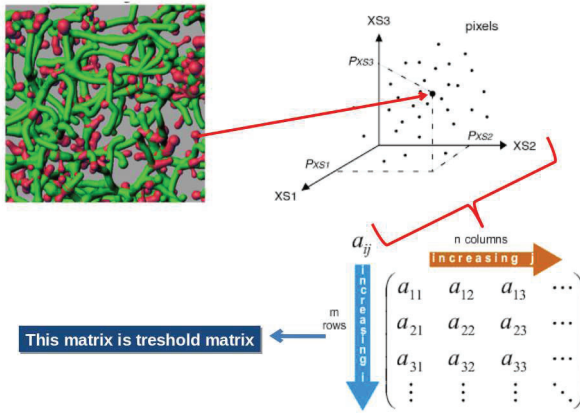


Figure 4.16: Reduced spine density of neurons after 12 weeks of cosmic radiation.

Our approach was the following: One may use these images to regionalize dendrites and spines and get, by using the Voronoi diagrams, some adjacent areas where spines and dendrites are concentrated. Once, the centers of the adjacent areas are connected, we get a Delaunay diagram which yields to a Rips complex on which TDA theory can be applied to get bare codes.

Firstly, to get the complex of Rips, we choose a threshold distance between the dendrites and spines region, that is the average distance between these regions for a graph exposed to 0cGy. With this threshold distance, we get a filtered graph which leads to a boundary matrix.

Secondly, we implement a matrix reduction algorithm to pair the persistent data, which represents the focus of cosmic radiation exposure. Finally, we calculate the diameter between two distant areas and compare to that obtained for another exposure to get a prediction tool of the different cosmic radiations from the different obtained diameters of two focus of dendrites-spines cliques). In what follows, we explain our approach step by step : **Step 1** : Get the adjacency matrix from an image (as explained by the image here below).



For this purpose we implemented the following algorithm:

Algorithm 5 Adjacency matrix.

Input: image
Output: matrix pixel threshold
 i, j =size of image
for u in i **do**
 for v in j **do**
 pixel=python_image_pixel
 if pixel == green or pink, **then**
 matrix_pixel(i, j)=1
 else
 matrix_pixel(i, j)=0
 end if
 end for
end for

Step 2: It consists to create the associated Voronoi diagrams by inserting the sites events in a file

Here above some images of the dendrite and spines repartition after a cosmic radiation and their associated Voronoi diagrams.

Algorithm 6 Voronoi diagrams.

```
while E is no empty do  
  withdraw a p event  
  if this event is a site then  
    create a new parabolic arc  
    create the Voronoi edge  
    delete the depraved circle event  
    insert circle events  
  end if  
  if this event is a circle then  
    delete parabolic arc  
    create the Voronoi vertex  
    delete the depraved circle event  
    insert circle events  
  end if  
end while
```

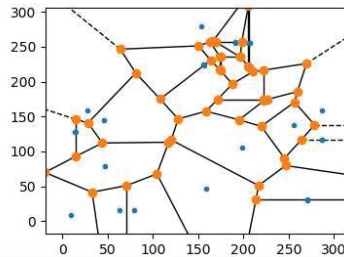
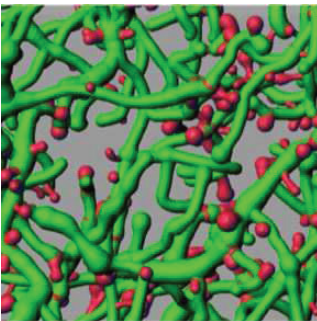


Figure 4.17: Voronoi diagram issued from a 5 cGy⁴⁸Ti radiation.

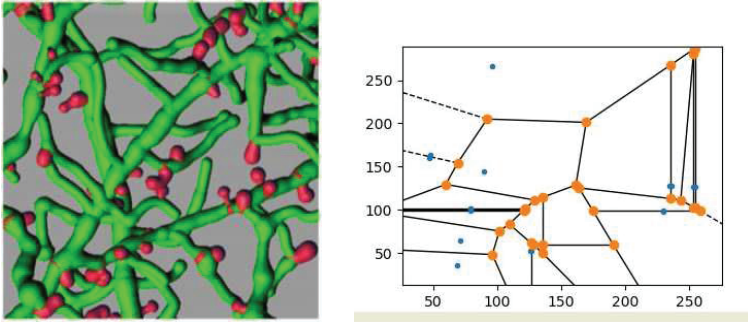


Figure 4.18: Voronoi diagram issued from a 30 cGy⁴⁸Ti radiation.

Step 3: Build a Deluanay complex from the recently constructed Voronoi diagram as outlined by the following picture:

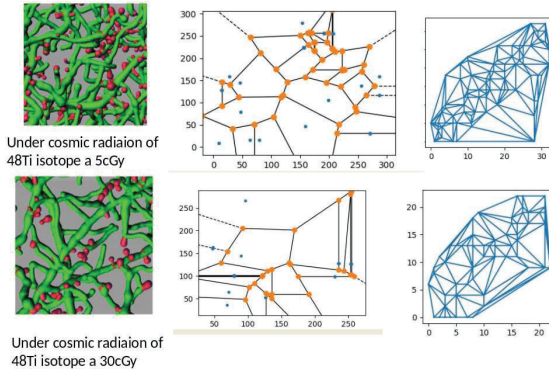


Figure 4.19: Examples of Delaunay complexes issued from Voronoi diagrams by using the Algorithm 7

Step 4: To build a Rips complex from the obtained Delaunay triangulation, we consider the Wasserstein distance in the following algorithm:

Step 5: The final step is to get the boundary matrix. The idea is that since for all $r_0 \geq r$, we have $\text{Rips}(N, r) \subset \text{Rips}(N, r_0)$, then $\mathcal{F} = \{\text{Rips}(N, r), 0 \leq r \leq \text{rmax}\}$ is a filtration. This Rips filtration induces a boundary matrix as stated by the following algorithm:

Algorithm 7 Delaunay diagram

Input: Voronoi points
Output: Delaunay tessellation

```
for u from 0 to  $n - 1$  do
  mnb=mostnearneighbor(u)
  rn=rightneighbor()
  while rn!=mnb and rn!=-1 do
    if rn==-1 then
      convexe[u]=1
      lneig=leftneighbor()
      if lneig!=-1 then
        get neighbor
      end if
      while lneig!=-1 do
        delaunay tessellation= neighbor
      end while
    end if
  end while
end for
```

Algorithm 8 Rips complex.

Input: Delaunay Graph
Output: Rips complex

```
 $j = 0, wass = r$   
 $i = 0, \text{Ball}(a[i]) == a[i]$   
bool receives true  
for  $i$  from 0 to  $n - 1$  do  
  while bool do  
    if  $d(a[i], a[i + 1]) \leq r$  then  
      add  $a[i + 1]$  to  $\text{Ball}(a[i], r)$   
    else  
       $r == d(a[i], a[i + 1])$   
      bool receives false  
    end if  
  end while  
end for  
Rips complex receives Ball
```

Algorithm 9 Boundary matrix.

Input: Rips complex
Output: boundary matrix
for i from 0 to $n - 1$ **do**
 for j from 0 to $n - 1$ **do**
 if $a[j] == \text{face of } a[i]$ **then**
 $M[i, j]$ receives 1
 else
 $M[i, j]$ receives 0
 end if
 end for
end for

Finally to pair birth and death of cycles as early mentioned, we index columns by j , and $i = \ell(j)$ denotes the line that contains the lowest one in the column j , denoted C_j . A matrix is called *reduced*, when no two different columns have their lower at the same level. To get a reduced boundary matrix, we appeal this algorithm:

Algorithm 10 Boundary matrix.

Input: Boundary Matrix
Output: pairs (i, j)
for $j = 0..m$ **do**
 for $j' < j$ **do**
 while $\ell(j') == \ell(j)$ **do**
 $C[j] = C[j] + C[j'] \bmod(2)$
 end while
 end for
 draw $(\ell(j), j)$
end for

The fruit of this implementation is the following persistent diagrams

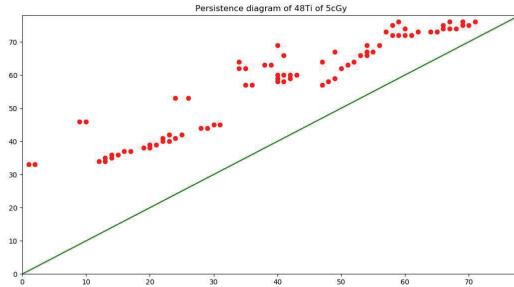


Figure 4.20: Persistent diagram that represents the dendrite and spines density under 5 cGy⁴⁸Ti radiation.

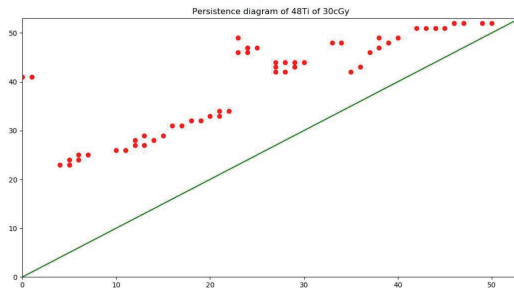


Figure 4.21: Persistent diagram that represents the dendrite and spines density under 30 cGy⁴⁸Ti radiation.

Our persistent diagrams show clearly how much the 30 cGy⁴⁸Ti radiations damage deeply neuronal tissue more than the 5 cGy⁴⁸Ti radiations. This shows the power of the topology approach in the data analysis. Indeed, the experiences led by the Limoli staff (as outlined here below) were unable to differentiate the negative effects on the neuronal tissue after radiation 5 cGy⁴⁸T and 30 cGy⁴⁸T.

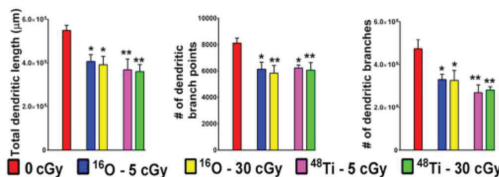


Figure 4.22: Dendrite density under different radiations.

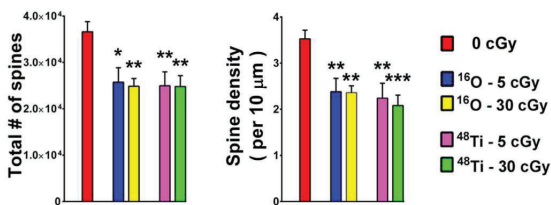


Figure 4.23: Spines density under different radiations.

5

Machine learning

Machine learning is an artificial intelligence technology that allows computers to perform tasks without having been explicitly programmed. For this purpose, they need data to analyse and train on. The aim in Machine learning is to discover patterns and make predictions from big data based on statistics, data mining, pattern recognition and predictive analytic. For example, based on some bank transaction information like the amount or the localization, and analysing the account history data, machine learning is useful to detect potential fraud in a millisecond. The Machine learning machinery consists of extracting information from big data sources: The more data injected into a machine learning system, the more this system can learn to discover the hidden patterns in the data with more efficiency.

Deep Learning is a machine learning example of application in visual recognition. For example, an algorithm will be programmed to detect certain faces from images coming from a camera. Depending on the database assigned, it will be able to spot a wanted individual in a crowd, detect the satisfaction rate when leaving a store by detecting smiles, etc. A set of algorithms will also be able to recognize voice, tone, expression of questioning, affirmation, and words.

Deep Learning is based on the concept of artificial neural networks: inspired by neurons in the human brain, we are made up of several artificial neurons connected to each other. The higher number of neurons is, the "deeper" network is. As signals travel between neurons, the neural network assigns a certain weight to different

neurons: A neuron that receives more load will exert more effect on adjacent neurons. Let us take a concrete example of image recognition: the goal is to recognize photos that contain at least one cat. In order to achieve this, the neural network has to compile a set of thousands of photos of different cats, mixed with images of objects that are not cats. These images are then converted into data and transferred over the network. The artificial neurons then assign a weight to the different elements. The final layer of neurons will then bring together the different information to deduce whether or not it is a cat.

Hence, TDA and machine learning share a common point: using and analysing big data. That was our key inspiration to attack, with a TDA angle of view, the famous open problem in machine learning, namely the "Bongard Problems". There is a set of 100 visual puzzles posed by M. M. Bongard, where each puzzle consists of twelve images separated into two groups of six images. The task is to find the unique rule separating the two classes in each given problem. The problems were first posed as a challenge for the AI community to test machines ability to imitate complex, context-depending thinking processes using only minimal information. Although some work was done to solve these problems, none of the previous approaches could automatically solve all of them. Our approach to attack these problems was to combine the tools of persistent homology alongside machine learning methods by implementing algorithms that are able to solve some problems involving differences in connectivity and size.

Bongard Problems [3] consist of twelve boxes, six of which follow a certain rule while the other six break that rule. The task of the problem solver is to identify the underlying pattern. The following figure is an example of such a problem

Bongard Problems are not only a challenge for the AI community, they can also be helpful for engineers as well as mathematicians to understand and model brain functions such as learning, finding similarity, creating abstract ideas and acting by intuition. A machine that is able to solve Bongard Problems is indicative of the presence of high-level cognitive functions that can be further used to solve problems that go beyond the original posed problems such as retrieving similar images, finding a network of people with similar in-

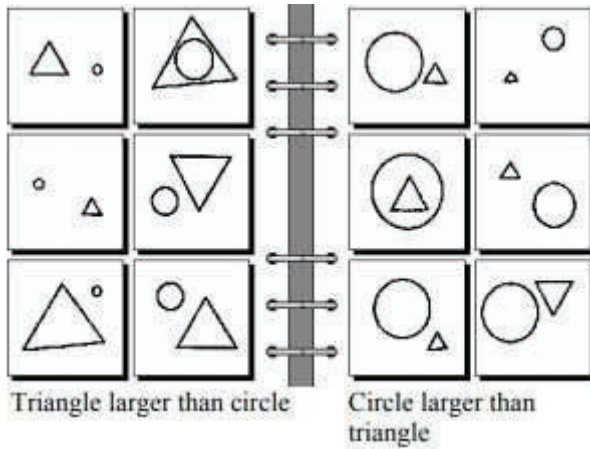


Fig. 4.24. Bongard Problem N°2.

terests, counting objects in images and videos or annotating images. Few efforts have been made to automatically solve Bongard Problems. Some major attempts are "RF4" by Saito and Nakano[63] and "Phaeaco" by Harry Foundalis [23]. They could solve in this way 10 of the 100 Bongard Problems.

We approached Bongard Problems from a different angle and considered ones that have not been solved by any of the systems mentioned earlier (see [6]). The topological tool, as far as we know, has never been used to attack these problems. The central idea in our work was to find the pattern setting apart the two classes of shapes in each Bongard Problem. Homology groups formalize the description of the topology of geometric objects, specifically, persistent homology gives us a way to make that distinction by means of comparing topological signatures.

For our purpose to resolve Bongard Problems, we assume that images can be studied and compared through their topological signatures. We also assume that given the right feature function along with the right clustering parameters, it is possible to find a grouping that matches perfectly the one in the original problem.

The algorithm takes as input the 12 images as well as their corresponding classes. The proposed algorithm consists of four main steps. We first select a feature to compute from a pre-determined set

of features. We then perform image clustering based on that feature. If the resulting clustering matches the original one, there is a high chance that the feature used for the clustering is the rule of interest. Otherwise, we select another feature and go through that same process again. At the end, we can get one of two outcomes: either we find the separating rule or the time is out. We can circumvent the latter issue by both automatically extending the feature set and optimizing the algorithm. We should note that this is out of the scope of the present paper. The figure and algorithm below summarize our approach entirely.

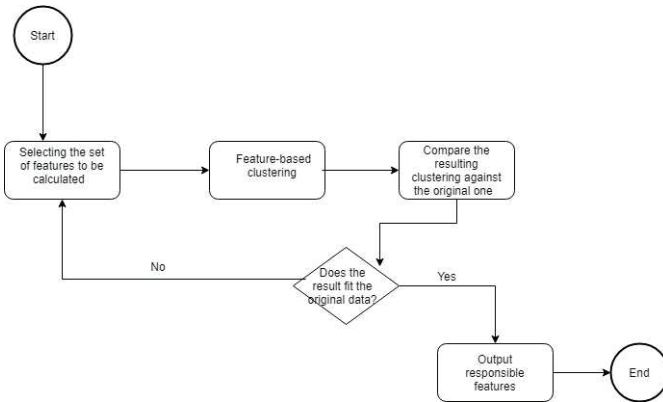


Fig. 4.25. Summarized Method.

For the first time, we used classical persistent homology to resolve Bongard Problem N° 23 by computing persistence diagrams of the images, and then transforming them into persistence images and then feeding them to the clustering algorithm before deciding if the number of components is actually the separating rule.

Algorithm 11 Abstract General Algorithm.

Input: 12 Bongard images with corresponding class

Output: The separating feature/rule

while not all feature functions are called **do**

 feature \leftarrow random feature call

 cluster \leftarrow images based on feature

 match \leftarrow compare original and resulting clusters

end while

if match is perfect **then**

 feature

else

 "solution not found"

end if

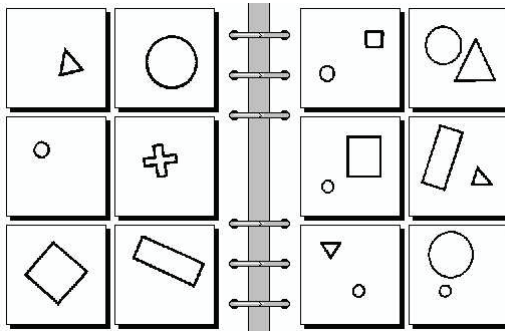
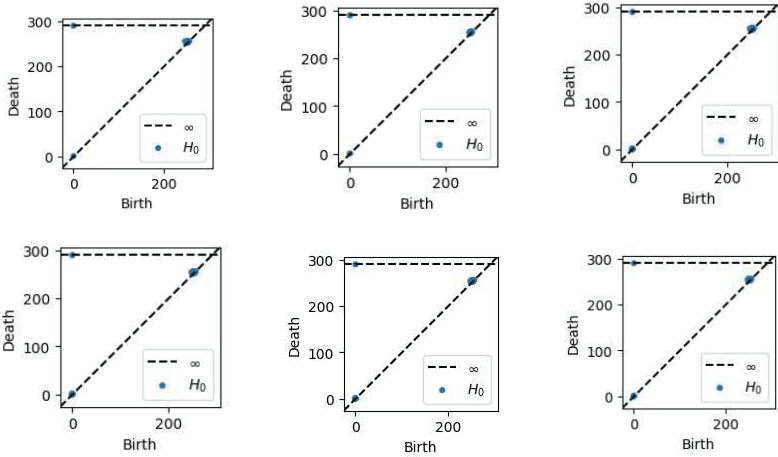
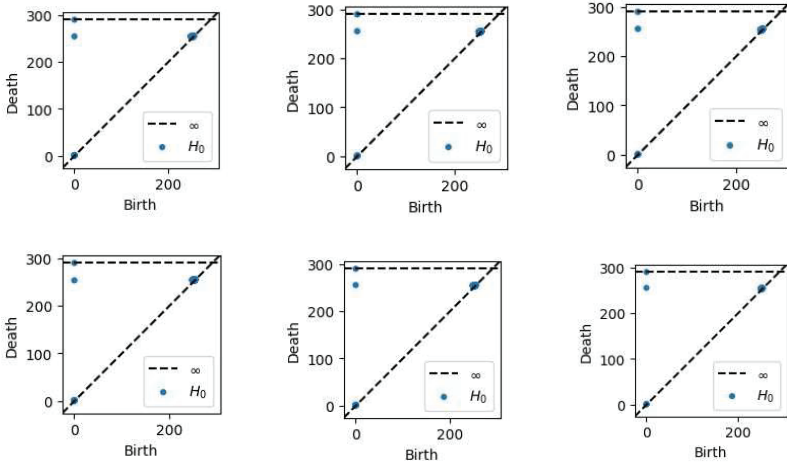


Figure 4.26: Bongard Problem N° 23.

Using the Ripser library, we compute the 0-dimensional lower star filtration on each of the twelve images. We get the following results:



(a) Persistence Diagrams of left images

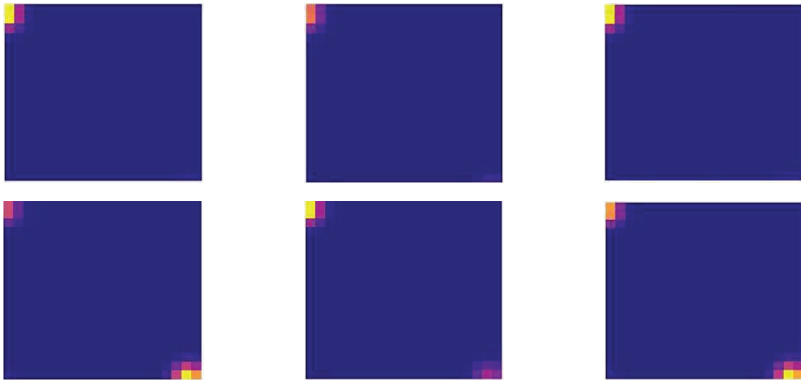


(b) Persistence Diagrams of right images

Figure 4.27: Computed Persistence Diagrams

Unfortunately, it is hard to directly use persistence diagrams for machine learning tasks. Persistence images, on the other hand, are

well suited for that purpose. These are actually finite -dimensional vector representations of persistence diagrams. They too verify stability with respect to small perturbations. We get the following results using the Persim library.



(a) Persistence Images of left images



(b) Persistence Images of right images

Figure 4.28: Computed Persistence Images.

We clustered images using the DBSCAN algorithm on the basis of the *connex* function output (see Algorithm 12). The most important parameters to set are the minimum number of samples in each cluster and the ϵ parameter that determines the maximum distance between two samples to be considered as neighbours. In this case, the

ϵ parameter is set to 2. Since the twelve images should be separated into two classes of six images each, we set the minimum number of samples parameter to 6.

Algorithm 12 Sample feature functions.

Input: 12 Bongard images

Output: Persistent diagrams

Connex(image)

Convert image to grayscale image

Construct lower star image

Compute H_0

Compute persistence diagram

Transform persistence diagram to persistence image

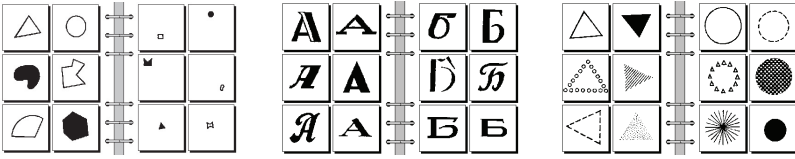
return persistence diagram

return persistence image

By computing the adjusted random index, we verify the match between the resulting and the original groupings. A perfect matching score indicates that the difference between the two sets of images resides in the number of connected components. It is the separating rule we are looking for.

The most important parameters to set are the minimum number of samples in each cluster and the ϵ parameter that determines the maximum distance between two samples to be considered as neighbours. In this case, the ϵ parameter is set to 2. Since the twelve images should be separated into two classes of six images each, we set the minimum number of samples parameter to 6.

The precedent classical persistent homology does not fit for other Bongard Problems. The above problems presents homeomorphic objects that cannot be separated using persistence diagrams in the classical form.



(a) Bongard Problem N°2.

(b) Bongard Problem N°100.

(c) Bongard Problem N°97.

For example, a solver that relies on such an approach would not make the difference between a triangle represented with straight lines and one represented with curved lines as in the case of Bongard Problem N°10. The Bongard Problems we are presenting next have not been solved by either approach. In almost of these problems instances, shapes in each group present similarities that cannot be captured using literal concepts.

In this setting, the use of G -equivariant non expansive operators presents itself as a better alternative to compare shapes and detect the rule of interest. Indeed, as stated earlier, one way of getting topological summaries of data is by building sublevel set filtrations on top of that data and computing persistence diagrams. However, persistent homology in the form we described cannot distinguish between summaries produced by a filtering function f and a filtering function $f \circ g$ when g is a self homeomorphism. That being the case, only a few Bongard Problems would benefit from the use of classical persistent homology when the invariance group is the group of all self-homeomorphisms, which we'll denote $Homeo(X)$. Other problems would better make use of invariance with respect to proper subgroups of $Homeo(X)$.

Our major source of inspiration in that regard was the Frosini et al. works [11] and [9]. Our main effort was to explore the possibility of using their results in the case of Bongard Problems, by being interested in the invariance with respect to previously chosen subgroups G of $Homeo(X)$ and then applying G -equivariant non-expansive operators g (see Definition 4.2) on filtrations to get multiple measurements associated with each filtration. These measurements can be thought of as different 'lenses' through which we see our data. We then approximate the natural distance between measuring functions

and construct a distance matrix which is then fed to the clustering algorithm. The subgroup G of $Homeo(X)$ transforms the set Φ of filtering functions by a right group action

$$f: \Phi \times G \rightarrow \Phi$$

$$(\varphi, g) \mapsto \varphi \circ g$$

Definition 4.2

Let Φ be a topological subspace of $C^0(X, \mathbb{R})$, the set of admissible filtering functions on X , and G a subgroup of $Homeo(X)$. F is a G -equivariant non-expansive operators if it verifies the following properties:

- F is a function from Φ to Φ ;
- $F(\varphi \circ g) = F(\varphi) \circ g$ for every $\varphi \in \Phi$ and every $g \in G$;
- $\|F(\varphi_1) - F(\varphi_2)\|_\infty \leq \|\varphi_1 - \varphi_2\|_\infty$ For every $\varphi_1, \varphi_2 \in \Phi$.

As previously said, computing the bottleneck distance between two persistence diagrams is not well suited for some problems in shape comparison, hence the need to introduce a G -bottleneck distance as a more powerful approach in comparing two filtrations.

Definition 4.3

The G -bottleneck distance with respect to a group G is defined by

$$d_G(\varphi_1, \varphi_2) = \inf_{g \in G} \max_{x \in X} |\varphi_1(x) - \varphi_2(g(x))|$$

Unfortunately, this distance presents a challenge; it is difficult to compute. To address this issue, we introduced $\mathcal{D}_{match}^{\mathcal{F}}$ as a tool to approximate d_G , which is also a G -invariant pseudo-metric on Φ

Definition 4.4

Let $\mathcal{F}(\Phi, G)$ be the set of all G -equivariant non expansive operators and \mathcal{F} be a non empty subset of $\mathcal{F}(\Phi, G)$

$$\mathcal{D}_{match}^{\mathcal{F}}(\varphi_1, \varphi_2) = \sup_{F \in \mathcal{F}} d_{match}(r_k(F(\varphi_1)), r_k(F(\varphi_2))).$$

For every $\varphi_1, \varphi_2 \in \Phi$. d_{match} corresponds to the bottleneck distance and r_k denotes the k -th persistent Betti number function with respect to the function φ .

The algorithm below describes our method.

Algorithm 13 G -Equivariance method.

Input: 12 Bongard images

Output: Distance Matrix

Equivariance(image)

operators \leftarrow list of operators

for img in images **do**

 lower_star_image \leftarrow compute lower star filtration of img

 apply list of operators on lower_star_image

for all pairs of lower_star_image with the same applied operator
 do

 Approximate the natural pseudo distance

end for

end for

Compute distance matrix

return Distance Matrix

The problems at hand are of geometric and topological nature. In this context, capturing geometric features and topological shape invariants makes sense. These invariants serve as candidates for the separating rule we are looking for. Once we compute the selected features, we transform them into a suitable format. We then feed them as input to a clustering algorithm (Algorithm 13) to separate the given data into regions of high density and others of low density. Once we have a known clustering solution, we have a ground truth clustering against which we can evaluate our results. If the resulting and original clustering match, the features responsible for that outcome are traced back and given as output.

For such cases, persistent homology and G -equivariant operators present powerful tools mainly for two reasons: firstly, because persistent homology can separate relevant features from noise and is more concerned with the general shape of data, and secondly, because GENEOs present the algorithm with multiple functions through which to see the data, thus giving it more ability to recognize the possible pattern governing the sets of images.

Letting G be the group of all similarity transformations, we can construct G -equivariant non expansive operators which serve as tools to identify images with similar patterns and arrange Bongard images into clusters that match the original ones.

The algorithm we proposed in this paper works in the same fashion. The algorithm constructs different representations of the same images, through the use of persistent homology summaries and G -equivariant non-expansive operators, allowing it to view the images using different 'lenses', the choice of the property that might explain the separation of the two sets is made at random. Performing clustering based on the chosen property and matching it with the original grouping allows the algorithm to decide if the separating rule was found.

6

Linguistics

If writing and talking are both tools for transmitting messages, writing has the advantage of being a reliable form of data storage that obeys the usual coding and decoding rules, which imply a shared understanding by the author and the reader of the sets of characters contained in the used writing system. Writing systems are a conventional visual mode to represent their oral communication. All writing systems require:

- symbols, individually called signs and collectively called writing;
- at least one set of rules and conventions (spelling) understood and shared by a community, which gives meaning to the basic elements (graphemes), their arrangement and their reciprocal relations;

- at least one language (generally spoken) whose constructions are represented and can be memorized by the interpretation of these elements and rules;

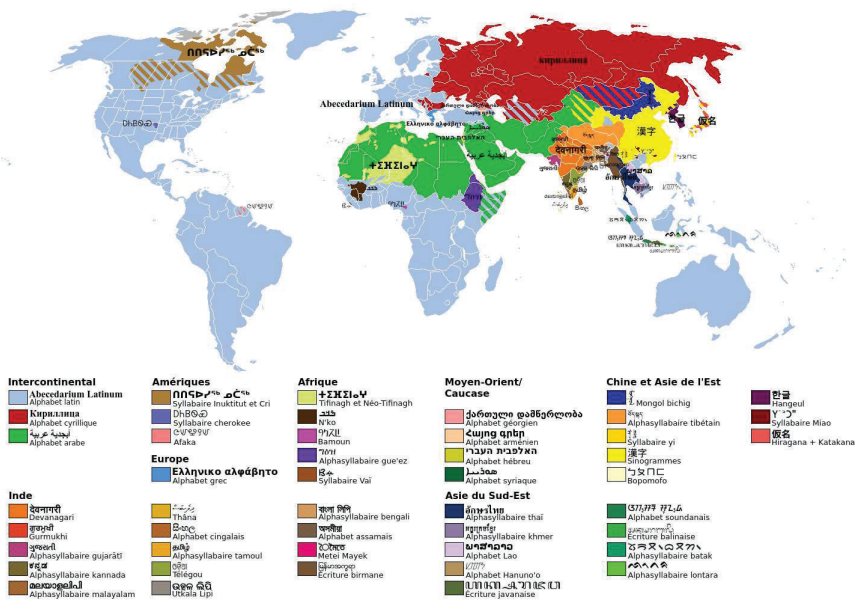


Fig. 4.30. Various written systems around the world.

We were interested in this folkloric linguistic research question: how to verify whether two writing systems are related. In fact, to demonstrate linguistic relatedness and to reconstruct a hypothetical common ancestral system of languages, linguists rely, among others, on the comparative method as a technique to study language development and perform comparisons on these languages (see [51]). However, the languages to compare are not chosen at random, and an initial stage of deciding whether some languages are related is required.

Tifinagh, which is the writing system we focused on in our work, is the script adopted for Tamazight or Berber languages more broadly. Berber have been originally spoken in territories ranging from the

Atlantic coast to Egypt before the arabization of North Africa. Millions of Tifinagh inscriptions of various styles and eras tattoo the rocks of North Africa and the Sahara. It is at the end of a long process of cultural and identity changes that begun with the emergence of Islam in the seventh century, that the Maghreb will be born. Concurrently, the linguistic map of Tifinagh (see FIGURE 6) retracts over the centuries until its present form, broken into islands distant from each other.

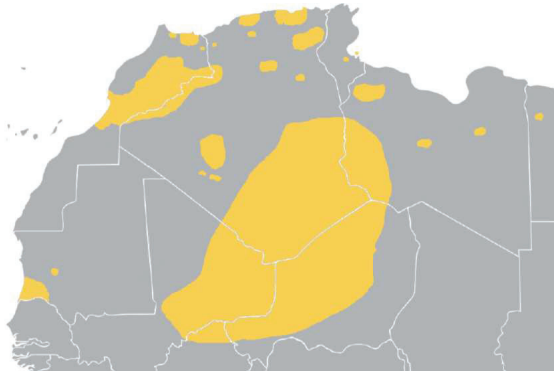


Figure 4.31: Current Tifinagh speaking map in Africa.

There is no conclusive theory so far about the origin of the Tifinagh script. The origins proposed (see [59]) range from Norway, Greece, to the south of France and the Indus Valley. Suggested ancestors are, among others, the Ugaritic cuneiform scripts or the Runic inscriptions. As for its emergence dates, they range from 30,000-16,000 years BC to 429 AD. Recent research has refuted most of these hypotheses, but the question of the origin of the Tifinagh script has no definitive answer yet. Most scholars seem to gather mainly around three possibilities:

- South-Semitic origin (Arabian and/or Latin scripts);
- North-Semitic origin (Phoenician and/or Punic);
- Independent invention with Phoenician influence.

We focused on this specific question: are the Tifinagh and Phoenician scripts related? Our approach may be extended to study the relatedness of any two other languages, and as such, serve as a first step

to the comparative method, at least to the extent where only letter shapes are considered.

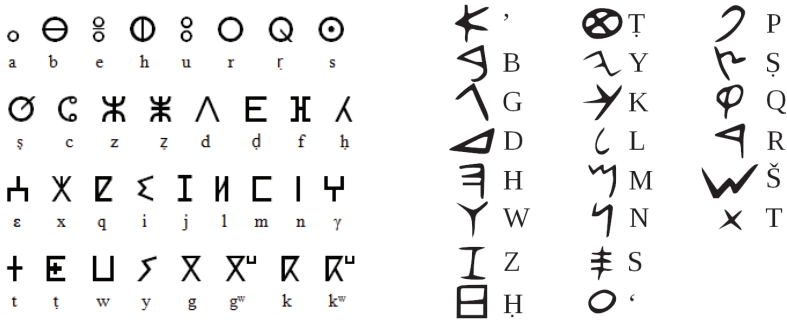


Figure 4.32: Left: Tifinagh scripts. Right: Phoenician scripts

To verify the relatedness of the two scripts, we adopt a topological data analysis approach based on persistent homology and graph theory. The letters of the writing systems we are studying are viewed as a graph. The topological information of interest in each of these graphs is summarised in persistence barcodes. Computing the Bottleneck distance between these topological signatures will serve as a means to verify similarity between Tifinagh and Phoenician scripts.

We define two scripts to be related, when we can get from one letter in one script to another one in the other script by a finite series of transformations. In order to model these transformations, we first represent each letter as a graph, or more specifically as a dynamical graph, by allowing operations such as adding or removing vertices and edges.

We will denote the set of Phoenician letters by \mathbb{P} and that of Tifinagh letters by \mathbb{T} . We summarize our approach in the following steps:

- Represent each letter in \mathbb{P} as a time-varying graph G ;
- Associate a metric space representation to each graph G and build a dynamical simplicial complex.

- Compute the zigzag persistent homology of G ;

We get the following:

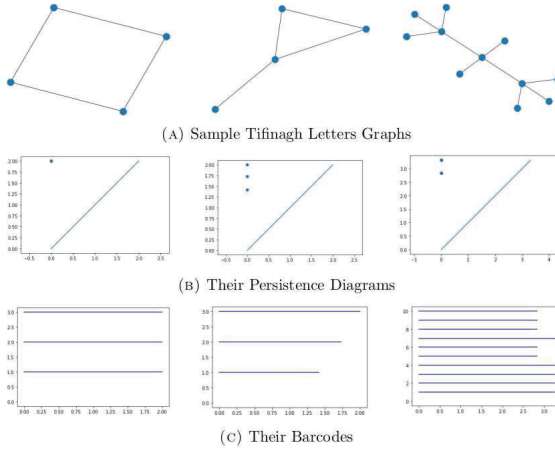


Figure 4.33: Tifinagh scripts TDA.

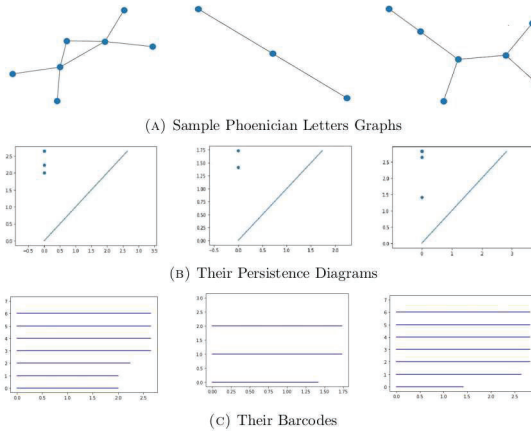


Figure 4.34: Phoenician scripts TDA.

Once this is done, the next step consists of making a clustering of \mathbb{P} and \mathbb{T} graphs on the basis of the pairwise bottleneck distances between their topological signatures in order to detect similarity between letters. Indeed, after computing the persistence diagrams associated to the simplicial complexes built on top of each graph, we compute the pairwise bottleneck distance between persistence diagrams. We obtain a distance matrix on the basis of which we perform hierarchical clustering, more specifically in this case an agglomerative clustering. Agglomerative clustering starts by considering each singleton as a cluster. The clusters are then inductively combined until some stop criterion is satisfied. In this work, the update at each step is performed using a complete linkage which measures inter-cluster dissimilarity based on the maximum distances between all data points.

We get the following:

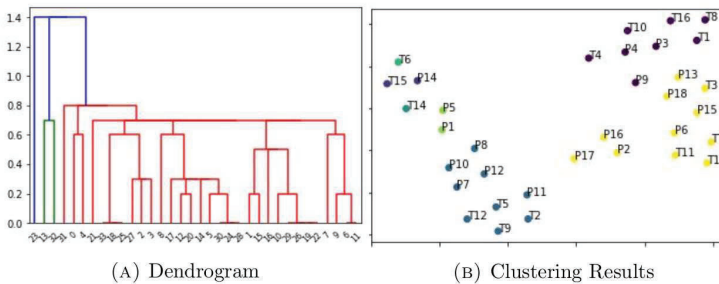


Figure 4.35: Tifnagh vs Phoenician scripts: Cluster repartition.

We see that, except for a few distinct points, each cluster in the right figure contains both Phoenician and Tifnagh letters suggesting similarity between the two. In this work, we demonstrated how TDA and persistent homology in particular can be used to verify the relatedness between two writing systems. Even though we restricted our analysis to the study of similarity between the Phoenician and Tifnagh scripts, the method we used can be extended to compare any

two writing systems. A future work might explore the nature of this relatedness i.e whether one script is derived from the other or one was built under the other's influence.

Chapter 5

Applied Category Theory

1 Glossary

In 2019, we switched to another exciting research area in applied algebraic topology, namely the Applied Category Theory (ACT for short) which is a relatively new branch of mathematics that has transformed much of pure math research. The technical advance is that category theory provides a framework in which to organize formal systems and by which to translate between them, allowing one to transfer knowledge from one field to another. But this same organizational framework also has many compelling examples outside of pure math. In fact, one of the great features of category theory is that its organizing principles have been used to reshape and reformulate problems within pure mathematics, including topology, homotopy theory and algebraic geometry. Category theory has shed light on those problems, making them easier to solve and opening doors for new avenues of research. Historically, category theory has found immense application within mathematics. We suggest to the reader, interested in learning more about ACT, the good and well written Spivak notes [22].

2

Dynamical systems (Ongoing Works)

Operads were introduced by May to describe compositional structures arising in algebraic topology [48]; Leinster has written a great book on the subject [46]. More recently, Spivak and his collaborators has discussed how to apply operads to model composition of structures in logic, databases, and dynamical systems (see [57], [67] and [68]). Actually we are working on some application in dynamical systems. We are especially interested in four open questions inspired by [44], [67] and:

1. The first is to investigate the mathematical properties of the wiring diagrams operad S (or T) and its algebras;
2. The second is to use the wiring diagrams operad and its algebras to study real-world phenomena;
3. The third is to change and expand the model, i.e. the operad S itself;
4. The fourth is to consider the category 2-cob of 1-dimensional oriented manifolds, and oriented cobordisms between them. 2-Cob is a symmetric monoidal category. You focus to try to prove the following: for every lax monoidal functor $2\text{-Cob} \rightarrow \text{Set}$, there is an associated traced monoidal category, where every object has been equipped with a commutative Frobenius structure.

Chapter 6

Bibliography

Bibliography

- [1] M. Amann. *A note on the Hilali conjecture*. In Forum Mathematicum. Vol. 29, No. 2 (2017) , 251-257. De Gruyter.
- [2] C. Allday, S. Halperin, *Lie group actions on spaces of finite rank*, Quart. J. Math. Oxford 28 (1978) 69-76.
- [3] M. M. Bongard. *Pattern Recognition*, Hayden Book Co., Spartan Books, Rochelle Park, N.J. (1970).
- [4] J. F. de Bobadilla, J. Fresán, V. Muñoz, and A. Murillo. *The Hilali conjecture for hyperelliptic spaces*. In Mathematics without boundaries, (2014) (21-36). Springer, New York, NY.
- [5] G. Bazzoni and V. Muñoz, *Rational homotopy type of nilmanifolds up to dimension 6*, arXiv: 1001.3860v1, (2010).
- [6] H. Bouazzaoui, M. I. Mamouni, M. A. Elomary. *Bongard Problems: A Topological Data Analysis Approach*. WSEAS TRANSACTIONS on SYSTEMS and CONTROL. Vol. 15 (2020). 131-140.
- [7] H. Bouazzaoui, M. I. Mamouni, M. A. Elomary. *Topological data analysis applied to writing systems*. Preprint (2021).
- [8] G. Carlsson. *Topology and data*. Bull. AMS, vol 46 (2009), 255-308.
- [9] F. Camporesi, P. Frosini, N. Quercioli. *On a new method to build group equivariant operators by means of permutants*. In International Cross-Domain Conference for Machine Learning and Knowledge Extraction (2018) 265-272. Springer, Cham.
- [10] M. Chas and D. Sullivan, *String topology*, preprint (1999) arXiv:math/9911159 [math.GT].

- [11] B. Di Fabio and P. Frosini. *Filtrations induced by continuous functions*, Topology and its Applications. Vol **160**, No. 12 (2013), 1413-1422.
- [12] H. Edelsbrunner, J. Harer, *Persistent homology: a survey*. Contemporary mathematics **453**(2008), 257-282.
- [13] B. B. El Krafi, M. R. Hilali, M. I. Mamouni. On Hilali's conjecture related to Halperin's. Journal of Homotopy and Related Structures, vol. 11, num 3 (2016), 493-501.
- [14] H. Edelsbrunner, D. Letscher, and A. Zomorodian. *Topological persistence and simplification*. Discrete Comput. Geom., vol **28** (2002), 511-533.
- [15] B. Ben El Krafi, M. I. Mamouni. *On the Theriault conjecture for self homotopy equivalences*. Rendiconti del Seminario Matematico della Università di Padova, Vol. **138** (2017), 209-221.
- [16] A. Ettaki, M. I. Mamouni, M. A. Elomary. *Applied category theory and circuit systems*. Preprint (2021).
- [17] M. Farber, *Topological complexity of motion planning*, Discrete Comput. Geom. vol. **29** (2003), no. 2, 211-221.
- [18] M. Farber, *Instabilities of robot motion*, Topology Appl. vol. **140** (2004), no. 2-3, 245-266.
- [19] M. Farber, M. Grant, *Symmetric motion planning*, Contemp. Math. , No. **438** (2007), 85-104.
- [20] Y. Félix and J.-C. Thomas, *Monoid of self-equivalences and free loop spaces*, Proceedings of the American Mathematical Society, Vol. **132** (2004), no. 1, 305-312.
- [21] Y. Félix, J.-C. Thomas. *String topology on Gorenstein spaces*, Math. Ann., Vol. **345** (2009), 417-452.
- [22] B. Fong, D. I. Spivak. *An invitation to applied category theory: seven sketches in compositionality*. Cambridge University Press (2019).
- [23] H. E. Foundalis. *Phaeaco: A Cognitive Architecture Inspired by Bongard's Problems*, Ph.D. Thesis, (2006).

- [24] Y. Derfoufi, M.I. Mamouni. *Motion planning algorithms, topological properties and affine approximation*. Bulletin of Computational Applied Mathematics, Vol. 3, No. 1 (2015), 7-12.
- [25] Y. Derfoufi, M.I. Mamouni. *Loop topological complexity*. Bulletin of Computational Applied Mathematics, Vol. 3, No. 2, (2015), 31-36.
- [26] Y. Derfoufi, M.I. Mamouni. *String topological robotics*. JP Journal of Geometry and Topology, Vol. 19 No. 3 (2016) 189-208.
- [27] T. Ganea, *Lusternik-Schnirelmann category and cocategory*, Proc. London Math. Soc., Vol. 3, Issue 10 (1960), 623-639.
- [28] M. Grant, G. Lupton, J. Oprea, *Spaces of topological complexity one*, Homology Homotopy Appl., Vol. 15, Num. 2 (2013), 73-81.
- [29] A. Hatcher. *Algebraic topology*, Cambridge University Press (2002).
- [30] S. Halperin, *Rational Homotopy and Torus Actions, Aspects of Topology*, ed. I.M. James and E.H. Kronheimer, London Math. Soc. Lecture Notes Ser. 93, 1985.
- [31] S. Halperin, *Finiteness in the minimal models of Sullivan*, Trans. Amer. Math. Soc. 230 (1983) 173-199.
- [32] M.R. Hilali, *Action du tore \mathbb{T}^n sur les espaces simplement connexes*, Thesis, Univ. catholique de Louvain, Belgique, 1990.
- [33] M. Hopkins, *Formulations of cocategory and the iterated suspension*, Astérisque, vol. 113-114 (1984), 212-226.
- [34] M. Hovey, *Lusternik-Schnirelmann cocategory*, Illinois Jour. of Maths., Vol. 37, Num. 2 (1993), 224-239.
- [35] M. R. Hilal, M.I. Mamouni, H. Lamane. *Classification of rational homotopy type for 8-cohomological dimension elliptic spaces*. Advances in Pure Mathematics, Vol. 2, No. 01 (2012), 15-21.
- [36] M.R. Hilali, M. I. Mamouni. *A lower bound of cohomologic dimension for an elliptic space*. Topology and its Applications, Vol. 156, No 2 (2008), 274-283.

- [37] M.R. Hilali, M. I. Mamouni, *A conjectured lower bound for the cohomological dimension of elliptic spaces*, Journal of Homotopy and Related Structures, Vol. **3**, No. 1 (2008), 379-384.
- [38] M. R. Hilali, M. I. Mamouni, J. Tarik. *On the rational homotopy type when the cohomological dimension is 9*. JP Journal of Geometry and Topology, Vol. **17**, No.2 (2015), 157-172.
- [39] M.R. Hilali, M.I. Mamouni and H. Yamoul. *On the Hilali conjecture for configuration spaces of closed manifolds*. African Diaspora Journal of Mathematics. New Series, Vol. **18**, No. 1 (2015) 1-11.
- [40] M.R. Hilali, M.I. Mamouni and H. Yamoul. *The rational homotopy type of elliptic spaces up to cohomological dimension 8*. Afrika Matematika, Vol. **27** No. 5-6 (2016), 851-864.
- [41] N. Iwase, M. Sakai, *Topological complexity is a fibrewise L-S category*, Topology and its Appl., vol **157**, no. 1 (2010), 10 -21.
- [42] N. Iwase, M. Sakai, *Erratum to Topological complexity is a fibrewise L-S category*, Topology and its Appl., vol. **159**, no 10-11 (2012), 2810-2813.
- [43] T. Kadeishvili, *Cohomology C_∞ -algebra and rational homotopy type*, arXiv:0811.1655v1 [math.AT] (2008).
- [44] J. Kock. *Frobenius Algebras and 2-D Topological Quantum Field Theories*. Cambridge University Press (2004).
- [45] F. Laudenbach, *A note on the Chas-Sullivan product*, L'Enseignement Mathématique, Vol. **57** (2011), Issue 1-2, 3-21.
- [46] T. Leinster. *Higher operads, higher categories*. London Mathematical Society Lecture Note Series. Vol **298** (2004). Cambridge University Press, Cambridge.
- [47] M.I. Mamouni. *String Topology Robotics 2*. Preprint (2021).
- [48] J.P. May. *The geometry of iterated loop spaces*. Lecture Notes in Mathematics, Vol. **271** (1972).
- [49] J. R. Munkres. *Elements of Algebraic Topology*, Addison-Wesley, Redwood City, California (1984).

- [50] M.I. Mamouni, H. Chawqi. From digital images to barcodes. *International Journal of Advanced Trends in Computer Science and Engineering*, Vol. 9 No.(2020), 1952 - 1958.
- [51] A. McMahon, R. McMahon. *Language classification by numbers*. Oxford University Press on Demand (2005).
- [52] D. Quillen, *Rational homotopy theory*, *Ann. of Math.* **90** (1969), 205-295.
- [53] H. Poincaré, *Oeuvres complètes*. Volume 6 (1953), Gauthier Villiar, Paris, France.
- [54] V.K Parihar, B. D. Allen, K. K. Tran, T. G. Macaraeg, E. M. Chu, S. F. Kwok, N. N. Chmielewski, B. M. Craver, J. E. Baulch, M. M. Acharya, F. A. Cucinotta and Ch. L. Limoli. *What happens to your brain on the way to Mars*, *Life Sciences in Space Research*. Vol. **1**, no. 4 (2015), 1-6.
- [55] V. K. Parihar and Ch. L. Limoli. *Cranial irradiation compromises neuronal architecture in the hippocampus*. *PNAS*, Vol. **110** , no 31 (2013), 12822-12827.
- [56] V. K. Parihar , B. D. Allen, Ch. Caressi, S Kwok, E. Chu, K. K. Tran, N. N. Chmielewski, E. Giedzinski, M. M. Acharya, R. A. Britten, J. E. Baulch and Ch. L. Limoli. *Cosmic radiation exposure and persistent cognitive dysfunction*, *Scientific Reports*, Vol. **6** (2016), 34774-34788.
- [57] D. Rupel, D. I. Spivak. *The operad of temporal wiring diagrams: formalizing a graphical language for discrete-time processes*. eprint: arXiv: 1307.6894 (2013).
- [58] M. Sbaï, *La cocatégorie rationnelle d'un espace*, Thèse de 3ème cycle, Univ. Lille, France (1984).
- [59] W. Pichler. *The origin of the Libyco-Berber script*. In Actes du colloque international Le libyco-berbère ou le tifinagh: de l'authenticité à l'usage pratique (2007), 153-186.
- [60] D. Sullivan, *A General Problem*. In "Proc. 1970 Amsterdam Conference on Manifolds", *Lecture Notes in Math*, No. **197** (1970), Springer.

- [61] D. Sullivan, *Infinitesimal computations in topology*, Publ. I.H.E.S **47** (1977), 269-331.
- [62] D. I. Spivak, P. Schultz, D. Rupel. *String diagrams for traced and compact categories are oriented 1-cobordisms*. arXiv:1508.01069 [math.CT]
- [63] K. Saito, R. Nakano. *Adaptive concept learning algorithm: Rf4*. Trans. of IPSJ, **Vol. 36**, No 4 (1995), 832-839.
- [64] M. Schlessinger and J. Stasheff, *Deformation theory and rational homotopy type*, arXiv:1211.1647v1 [math.QA] (2012).
- [65] H. Shiga and T. Yamaguchi, *The set of rational homotopy types with given cohomology algebra*, Homology Homotopy and Applications, **Vol. 5**, No. 1, (2003), 423-436.
- [66] H. Shiga and N. Yagita, *Graded algebras having a unique rational homotopy type*, Proc. of the A.M.S, **Vol. 85**, No. 4, (1982), 623-632.
- [67] D. I. Spivak. *The operad of wiring diagrams: formalizing a graphical language for databases, recursion, and plug-and-play circuits*. eprint: arXiv:1305.0297 (2013).
- [68] D. Vagner, D. I. Spivak, E. Lerman. *Algebras of open dynamical systems on the operad of wiring diagrams*. In: Theory and Applications of Categories, **Vol. 30**, No. 51 (2015), 1793-1822
- [69] Whitehead, G. W. (2012). *Elements of homotopy theory* (Vol. 61). Springer Science & Business Media.